Elementary processes and x-ray spectra of multiply charged ions in dense high-temperature plasmas

A. V. Vinogradov, I. Yu. Skobelev, and E. A. Yukov

P. N. Lebedev Institute of Physics, Academy of Sciences of the USSR, Moscow
Usp. Fiz. Nauk **129**, 177–209 (October 1979)

X-ray spectroscopic methods have been increasingly used in recent years in studying dense high-temperature plasmas produced by sources relying on the vacuum spark, the plasma focus, laser-beam or electron-beam interactions, and exploding wires. The plasma produced in such sources is usually in a state that is intermediate between thermodynamic and coronal equilibrium so that the intensities in the spectra of multiply-charged ions are largely determined by the kinetics of excited-state relaxation. An analysis is given of the methods available for calculations of cross sections and rates of relaxation of excited states under electron and ion impact. The relative intensities of x-ray lines and their possible use in plasma-density diagnostics are examined. The effects of electric and magnetic fields in plasmas on line spectra of multiply-charged ions are briefly discussed.

PACS numbers: 52.70. – m, 52.20. – j, 52.25.Ps

CONTENTS

1. INTRODUCTION

The advent of pulsed heating and inertial confinement of plasmas has opened up new possibilities for research into the dynamics of dense[1)] high-temperature plasmas and of atomic processes involving multiply-charged ions in such plasmas.

The rapid development of laser plasma research (see Refs. 1–7) has led to proposals for and experiments on the utilization of high-intensity electron[8–11] and ion[12–16] beams in producing the conditions necessary for thermonuclear reactions. According to current ideas, plasmas can be produced by focusing high-power photons or charged-particle pulses on the surface of solid targets. Moreover, the use of composite targets and of pulses of the appropriate shape should, at least in principle, produce compression of the target material by a factor of about 10^2–10^4 as compared with the solid-state density, so that the Lawson criterion $n\tau \sim 10^{14}$ cm^{-3} sec should be much more readily satisfied (n is the plasma density and τ is its lifetime).

Progress in this field has presented theoretical and practical spectroscopy with new problems because line spectra are among the few and, at the same time, most informative sources of data on processes occurring in dense hot regions.

The point is that it is practically impossible to use contact diagnostics for inertially confined plasmas in which the most important processes occur over time intervals $\sim 10^{-8}$–10^{-9} sec and over distances $\sim 10^{1}$–10^{3} cm. Interferometric methods, the probing of plasmas with laser beams, and laser scattering, which have been widely used in systems with magnetic plasma confinement (see Refs. 17–19 and the references cited therein), are still restricted to electron densities $N_e \leqslant 10^{20}$ cm^{-3}. Successful application of these methods in active diagnostics of plasmas with electron densities $N_e > 10^{22}$ cm^{-3} will require a substantial reduction in the wavelength of the probing laser radiation (down to 1000 Å or less). The development of lasers with the necessary angular and spectral characteristics in this wavelength

[1)] The phrase "dense plasma" is meant to represent plasmas with electron density $N_e \gtrsim 10^{19}$ cm^{-3}.

 0038-5670/79/100771-17$01.10

band is an independent problem that is still far from final solution (see, for example, Refs. 20–22).

On the other hand, x-ray spectroscopy has now reached a stage where spectra can be examined with spatial resolution down to 10 μ (Ref. 23) and time resolution of $\sim 10^{-9}$ (Refs. 24 and 25). There are practically no restrictions on electron density that are connected with refraction of the radiation or transparency of the plasma under investigation in the x-ray range. Theory thus faces the traditional problem, namely, analysis of the interaction between the particles and of the transport processes in plasmas with a view to extracting information on plasma parameters from observed characteristics of the spectrum.

The diagnostic problem formulated above awaits urgent solution in most of the plasma devices used for pulsed heating and inertial confinement of plasmas, including the vacuum spark, the plasma focus, exploding wires, and powerful laser and electron beams. Plasmas produced in such sources have high densities and are therefore unusually bright sources of x-ray line spectra. In recent years, studies carried out with such systems have stimulated research into further applications of the x-ray band and new methods for plasma diagnostics. The net result of all this has been the realization that existing data on fundamental atomic constants of multiply-charged ions, such as the wavelength of spectral lines, probability of radiative transitions, and collision cross sections, are clearly inadequate. The observed spectra could not be interpreted in the absence of reliable theoretical calculations of energy levels. In addition, the spectral line intensities could not be interpreted in the absence of detailed information on emission probabilities and collision cross sections. These quantities are exceedingly difficult to measure in the case of multiply charged ions so that theoretical data are the main sources of information.

On the other hand, comparison of observed and calculated spectra in a broad range of plasma parameters can provide information on the precision of atomic constants used in transport models of plasmas. This provides at least an indirect way of experimental verification of the basic assumptions used in the approximate solution of problems in atomic physics.

In this review, we shall consider the emission of spectral lines by hot dense plasmas (Chap. 2), the relaxation of excited states of ions (Chap. 3), the relative intensities of the spectral lines, and their possible use in plasma diagnostics (Chaps. 4–6). We shall also consider the influence of electric and magnetic fields on the emission spectra of multiply-charged ions (Chap. 7).

2. EXCITATION OF SPECTRA IN INERTIALLY CONFINED PLASMA

The character of the line spectrum emitted by an atom or ion depends on the conditions of excitation, i.e., in general, on all the physical parameters of the plasma that determine the distribution of the excited ions over the energy levels. When the rates of radiative and collisional transitions between the energy levels of ions are known, measurements of the relative line intensities can be used to determine the electron temperature T_e and the electron density N_e of the plasma. The pair of lines chosen for diagnostic purposes must be due to a sufficiently simple ion, so that the collisional relaxation constants and radiative transition probabilities can be determined theoretically with adequate precision, since experimental data on multiply-charged ions are almost totally lacking. Moreover, the lines must have sufficiently close frequencies in order to avoid difficulties with the calibration of the spectrograph. An excellent review of the state of this problem, mainly from the astrophysical point of view, has been given by Gabriel and Jordan.[26]

A substantial amount of new experimental data has accumulated in recent years on the x-ray spectra of ions in the vacuum spark,[27–31] the plasma focus,[32] the θ pinch,[33] the exploding wire,[34,35] and, especially, laser plasmas.[36–42] Figure 1 shows typical spectra recorded with crystal spectrometers for laser plasmas in the region 3–20 Å. Vacuum ultaviolet emission of laser plasmas with $\lambda \sim 100$–300 Å has been investigated with diffraction gratings at glancing incidence (Fig. 2). Typical spectrograms are shown in Figs. 3 and 4.

On the other hand, progress in the theory of atomic spectra[43–45] has led to the prediction of the energy levels of certain types of ion with spectroscopic precision. A large proportion of the observed lines in the spectra of ions belonging to the simplest isoelectronic sequences has been identified as the result of this. We therefore now have the completely realistic expectation that quantitative information on laboratory-plasma parameters will be determined from measured intensities of identified spectral lines in the x-ray band. This problem has

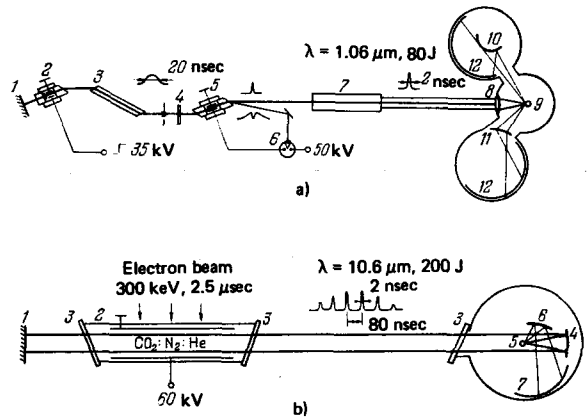

FIG. 1. Experimental arrangement for x-ray studies of laser plasmas.[137] (a) Heating of plasmas by neodymium laser: 1—100% mirror, 2—optical gate with quartz wedge polarizer, 3—active element, 4—16% output mirror, 5—optical gate with quartz wedge polarizers, 6—discharger with laser switching, 7—seven amplifiers (with output aperture of 60 mm in diameter), 8—focusing system, 9—target, 10—convex mica crystal ($2d = 19.8$ Å), 11—LiF crystal ($2d = 4$ Å) in the Couchoirs arrangement, 12—UF-VR x-ray film. (b) Heating of plasmas with CO_2 laser with plasma mirror: 1—flat gold-plated mirror, 2—laser cavity, 3—NaCl windows, 4—parabolic gold-plated mirror, 5—target, 6—crystal in Johann arrangement, 7—film.

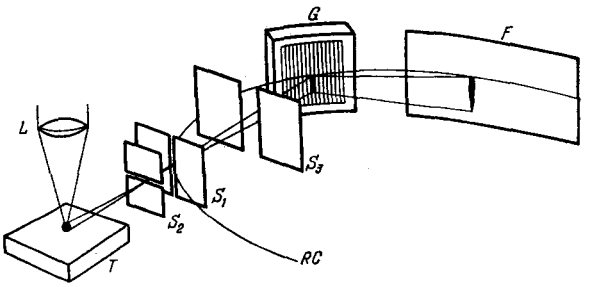

FIG. 2. Detection of vacuum UV radiation from laser plasma:[108] T—target, S_1—entrance slit of spectrograph, RC—Rowland circle, G—diffraction grating, F—photographic film, S_2—auxiliary slit producing the necessary spatial resolution in the direction away from the plane of the target.

been examined in detail in Refs. 46 and 47 in relation to the problem of determining the temperature and ionization state of plasmas. The determination of the electron density is no less important for applications and, in the first instance, for studies of inertially confined plasmas. The particular feature of laboratory plasma in this case is that the spectral line intensities depend on the probabilities of collisional transitions between excited states, i.e., in the final analysis, on the plasma density.

To illustrate the foregoing, consider a simple three-level scheme (Fig. 5), where the excited levels 1 and 2 are connected to the ground state 0 by radiative transitions with probabilities A_1 and A_2, respectively, and the rate of mixing of levels 1 and 2 by electron impact is,

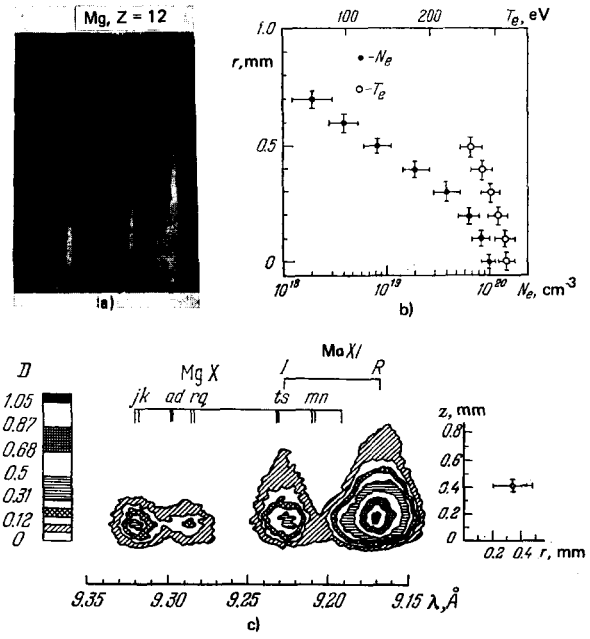

FIG. 3. (a) Spatially resolved spectrum of MgX and MgXI in the range 9.15–9.35 Å (Ref. 116). Plane of the target is at the bottom of the figure. There is a clear variation in relative intensity with distance r from the target. (b) Temperature and density profiles of plasma, deduced from the relative intensities in the spectra of MgX and MgXI. (c) Equal-density plots for the x-ray images of the laser facula. The scale of the image and the spatial resolution along the two coordinate axes are shown on the right; The density scale is shown on the left.

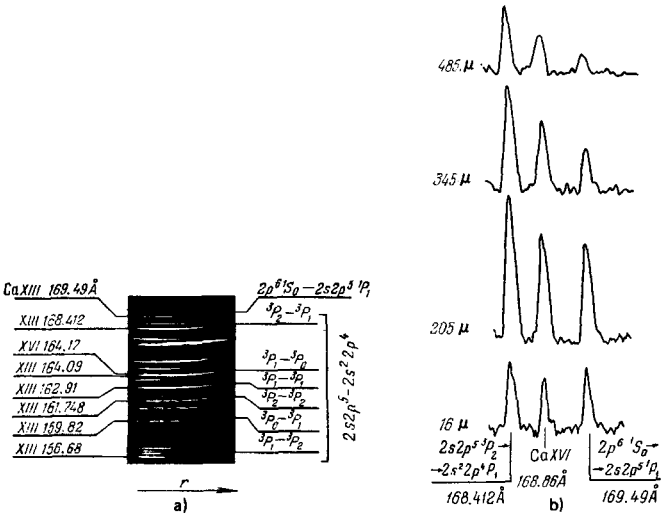

FIG. 4. Spectrum of CaXVI in the range 156–170 Å[108] (a); (b) shows density plots obtained for the spectra at different distances from the surface of the target. There is a clear variation with distance in the intensity ratio for the 168.412 and 169.49 Å lines, which depends on the plasma density (see Sec. 4D).

as usual, much greater than the rates of excitation from the ground state, $\langle v\sigma_{01}\rangle$ and $\langle v\sigma_{02}\rangle$. In the limitng cases of low and high plasma densities, the intensity ratio $\alpha = I_1/I_2 = N_1A_1/N_2A_2$ (N_1 and N_2 are the populations of levels 1 and 2, respectively) corresponds to the coronal and Boltzmann distributions, respectively. In the limit of low densities, when each excitation event is accompanied by a radiative decay, we have the coronal distribution and the intensity ratio is equal to the ratio of rates of excitation of levels 1 and 2, i.e., $\alpha = \alpha_C = \langle v\sigma_{01}\rangle/\langle v\sigma_{02}\rangle$. At very high densities, when collisional relaxation processes predominate over radiative processes, we have the Boltzmann distribution and the intensity ratio α becomes $\alpha_B = g_1A_1/g_2A_2$ (where g_1 and g_2 are the statistical weights of levels 1 and 2, respectively, and it is assumed that the difference between the energies of levels 1 and 2 is much less than the electron temperature). Depending on level structure, the values of α_C and α_B may be comparable in magnitude but may also differ by several orders of magnitude. It is clear that there is an intermediate range of values of the electron density N_e (Fig. 5), where the rates of radiative and collisional relaxation are of the same order, and the relative intensity α varies from α_C to α_B. It is precisely this region that is of main interest for plasma diagnostics. In particular, for the level scheme shown in Fig. 5, the region of appreciable dependence of α on

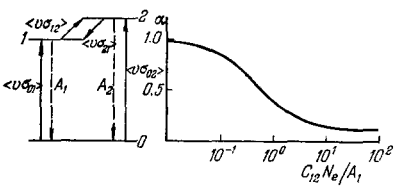

FIG. 5. Three-level model illustrating the origin of the density-dependent intensity ratio. The figure shows the function $\alpha(N_e)$ for the given model with $C_{01} = C_{02}$ and $g_1A_1 = 0.1g_2A_2$.

N_e corresponds to

$$N_e \gg \frac{A_1}{C_{12}} = \frac{A_1}{\langle v\sigma_{12}\rangle}. \tag{2.1}$$

Under astrophysical conditions, the inequality given by (2.1) can be satisfied only for metastable states connected by a forbidden transition to the ground state. Under laboratory conditions and, above all, for inertial methods of plasma confinement (laser plasma, high-intensity electron beams, and exploding wires), the condition given by (2.1) can be satisfied for allowed, and even for resonance, transitions.

The use of laser plasma as a source evidently provides a unique possibility of observing in a single experiment the lines of a particular ion emitted from regions differing in electron density by several orders. We thus have the possibility of direct observation of the transition from one mechanism of excitation of spectra to another and, consequently, a direct determination of the intensity ratio α as a function of the plasma density (Figs. 3 and 4).

In the next section, we shall consider some of the problems encountered in the evaluation of the atomic constants necessary for the determination of the function $\alpha(N_e)$. In the subsequent sections, we shall consider several pairs of lines corresponding to the $n=2\to n=1,2$ transitions (n is the principal quantum number) in H-, He-, and O-like ions for which measured intensity ratios can be used to determine the plasma electron density.

Before the function $\alpha(N_e)$ can be determined, we must have data on rates of elementary processes of three types, namely, (a) excitation from the ground state by electron impact (or, in the case of autoionization states, by electron capture), (b) radiative decay, and (c) collisional processes leading to transitions between excited states.

The necessity of studying processes (a) and (b) in the case of multiply charged ions arose in connection with a number of astrophysical problems. Intensive studies during the last decade have resulted in experimental data on these processes for ions with moderate degree of ionization,[48-55] and reasonably reliable theoretical values.[56-60]

There are practically no experimental data on multiply-charged ions in the case of the last of the above three types of process, whereas theoretical data are clearly inadequate. Several laboratories have developed detailed programs for studying the scattering of charged particles by ions, using detailed numerical calculations of atomic structures.[61-63] However, theoretical description of the spectrum requires not merely one or two but a large number (up to a few tens) of cross sections, and this presents considerable computational difficulties. In view of all this, the development of possibly less precise but simple and universal methods of calculating the necessary cross sections[58,64-66] remains an urgent problem for plasma diagnostics.

Before we proceed directly to the discussion of relaxation rates and intensity ratios, we note that levels 1 and 2 in Fig. 5 usually correspond to the same principal quantum number. The energy difference between these levels is, therefore, very small:

$$E_2 - E_1 \ll kT_e, \quad E_2 - E_1 \ll E_1, \quad E_2 - E_1 \ll E_2. \tag{2.2}$$

These inequalities lead to the following three important consequences: 1) when the rate of mixing by electron impact is calculated, effects associated with the Coulomb attraction between electrons and ions are not important; 2) inclusion of the Coulomb repulsion is essential in calculations of the rate of mixing by ion-ion collisions, and 3) the energy-level difference in dense plasmas may turn out to be of the order of the frequency of the electron Langmuir oscillations; if this is so, then, in general, Debye screening of the exciting electron (ion) by the charged plasma particles must be taken into account.

Thus, the first step in calculations of the rate of collisional mixing of excited states is to determine which particles (electrons or ions) are the most important, and then to calculate the rates of transfer in the light of the foregoing remarks.

3. RATES OF COLLISIONAL RELAXATION OF EXCITED STATES

Since the excitation energy $\Delta E = \hbar\omega = E_2 - E_1$ is small in comparison with the kinetic energy of the colliding particles, their relative motion can be regarded as classical, and we can use the impact parameter approach. The transition cross section $\sigma_{12}(v)$ is then given by

$$\sigma_{12}(v) = \int_0^\infty 2\pi\rho W_{12}(\rho, v)\, d\rho, \tag{3.1}$$

where $W_{12}(\rho, v)$ is the probability of the $1\to 2$ transition in a collision between the ion and the charged particle of relative velocity v and impact parameter ρ. The following point is important in calculations of the transition probability $W_{12}(\sigma, v)$ and the cross section $\sigma_{12}(v)$. The effect of Coulomb forces on the path of the colliding particles or, in other words, the extent to which the true path differs from the straight-line path is determined by the Coulomb parameter[67]

$$\nu = \frac{Z_1 Z_2 e^2 \hbar\omega}{M v^3}, \tag{3.2}$$

where $Z_1 e$ and $Z_2 e$ are the charges of the colliding particles, and M is their reduced mass. If we substitute the mean velocity $v_T = \sqrt{kT/M} = (Z_2/n_0)\sqrt{\theta/M}$ into (3.2) (where $\theta = kTn_0^2/Z_2^2\,\mathrm{Ry}$, $\mathrm{Ry} = 13.6$ eV, and n_0 is the principal quantum number of the ground state of the ion involved in the transition), we obtain

$$\nu = n_0 Z_1 \sqrt{\frac{M}{m\theta}}\,\frac{\Delta E}{kT}, \tag{3.3}$$

where m is the electron mass.

When the plasma is in ionization equilibrium, the parameter θ lies in the range $\sim 1/3 - 1/2$ and (3.3) shows that $\nu \ll 1$ for electron-ion collisions ($M = m$, $Z_1 = 1$) with small resonance defects ($\Delta E \ll kT$), so that the curvature of the paths of the colliding particles is un-

important.[67] On the contrary, in the case of ion-ion collisions, the formula given by (3.3) shows that the Coulomb parameter ν can be large even for $\Delta E \ll kT$, so that the repulsion between the ions must, in general, be taken into account. Accordingly, electron-ion and ion-ion collisions will be considered separately in the following two subsections.

A. Cross sections and transition rates for electron-ion collisions

As indicated above, the motion of the incident electrons can be regarded as taking place over straight line paths when the transition probabilities are calculated for electron-ion collisions.

The latent symmetry of the problem enables us to find the exact solution of the quantum-mechanical problem for the hydrogen atom in the field of a uniformly moving charge[68] if the off-diagonal radial matrix element for the interaction has the form

$$V(R)=\frac{\lambda}{R^2}, \tag{3.4}$$

where R is the separation between the incident electron and the nucleus. The scattering matrix for this problem was used in a number of papers on the theory of collisions and in the theory of broadening of spectral lines.[69-72] An analogous solution can also be used for optically allowed transitions in nonhydrogen-like atoms.

However, the potential given by (3.4) provides the correct description of electron-ion interactions only for large separations, because the true potential remains finite as $R \to 0$. It has been shown[73] that this ensures that the use of this potential leads to collision cross sections at high energies that are too large by a factor of at least two. It follows that the Born approximation with a potential correctly describing the interaction at small separations is better in the present case.

Shevelko *et al.*[74] used an off-diagonal potential for inelastic interactions in the form

$$V(R)=\lambda R\,(R^2+R_0^2)^{-3/2} \tag{3.5}$$

(λ and R_0 are atomic constants characterizing the strength and range of the interaction) to develop a simple method capable of yielding analytic expressions for the cross sections and rates of excitation of optically allowed transitions in the Born approximation. Detailed analysis and comparison with numerical calculations have shown that, in contrast to the previously used potential given by (3.4), the potential (3.5) gives the correct description of the cross section both at high and low (up to the cross section maximum) energies of the incident electron. Without going into details of the derivation, we shall merely reproduce the formulas for the cross sections and rates of excitation that are necessary for applications.[2)]

[2)] Here and elsewhere in this section, we use the atomic system of units.

The excitation cross section is given by

$$\sigma_{12}(v)=\pi\left(\frac{\lambda}{\omega R_0}\right)^2 g\left(\frac{\omega R_0}{v}\right), \tag{3.6}$$

where ω is the transition energy, and

$$g(S)=8S^2\left\{K_0(S)K_1(S)-\frac{S}{2}\left[K_1^2(S)-K_0^2(S)\right]\right\}$$
$$=\begin{cases}2\pi S^2\exp(-2S), & S\to\infty,\\ 8S^2\left(\ln\frac{1.114}{S}-\frac{1}{2}\right), & S\to 0,\end{cases}$$

where $K_0(S)$ and $K_1(S)$ are the Macdonald functions.

The rate of excitation is obtained by averaging (3.6) over the Maxwellian distribution of electrons with temperature T_e:

$$\langle v\sigma_{12}\rangle=8\sqrt{2\pi}\,\frac{\lambda^2}{\omega R_0}f(\alpha)=\frac{1.23\cdot 10^{-7}\lambda^2 f(\alpha)}{\omega R_0}\ (\mathrm{cm^3\ sec^{-1}}), \tag{3.7}$$

where $\alpha=\sqrt{T_e/m}\,(\omega R_0)^{-1}$, and

$$f(\alpha)=\frac{1}{\alpha^3}\int_0^\infty K_1^2\left(\frac{1}{\alpha x}\right)\exp\left(-\frac{x^2}{2}\right)\frac{dx}{x^3}$$
$$=\begin{cases}(\ln\alpha-0.321)/\alpha & \text{for } \alpha\to\infty,\\ (1.43/\alpha^{4/3})\exp(-2.38/\alpha^{2/3}) & \text{for } \alpha\to 0.\end{cases}$$

Figure 6 shows graphs of $g(S)$ and $f(\alpha)$, as reported by Shevelko *et al.*[74]

The constants λ (related to the oscillator strength f_{12} and the probability $A_{21}\,\mathrm{sec}^{-1}$ of radiative transitions) are, in general, given by

$$\lambda^2=\frac{Z_1^2 f_{12}}{2\omega}=\frac{1.55\cdot 10^{-11}g_2A_{21}Z_1^2}{g_1\omega^3}, \tag{3.8}$$

$$R_0=2\int_0^\infty P_1(r)P_2(r)\,r\,dr\Big/3\int_0^\infty P_1(r)P_2(r)\,dr, \tag{3.9}$$

where $Z_1=1$ is the charge of the incident particle (electron), g_i is the statistical weight of the i-th level, P is the atomic weight function, and $\int_0^\infty P^2dr=1$. In the case of transitions without a change in the principal quantum number $(n,l)\to(n,l+1)$ in a hydrogen-like ion, we have

$$\lambda^2=\frac{3n^2[n^2-(l+1)^2](l+1)Z_1^2}{4(2l+1)},\quad R_0=\frac{n^2}{Z_1}. \tag{3.10}$$

The formulas given by (3.6) and (3.7) were obtained within the framework of the Born approximation, the

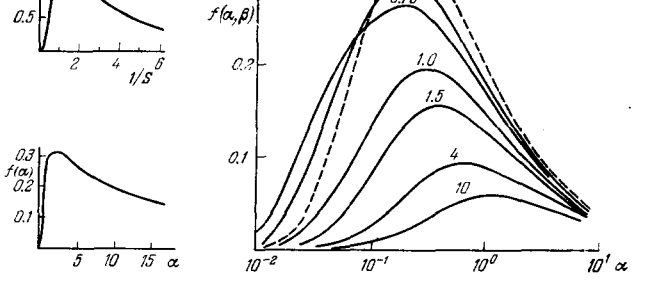

FIG. 6. Graphs of $g(S)$, $f(\alpha)$, and $f(\alpha,\beta)$, which determine the cross sections and rates of inelastic transitions occurring during electron-ion collisions. The function $f(\alpha,\beta)$ measures the influence of plasma effects on the inelastic collision frequency.

validity of which for transitions with a small resonance defect is (see Ref. 74 for further details)

$$\left(\frac{\lambda\omega}{v^2}\right)^2 \ll \frac{\omega R_0}{v} \ll 1. \tag{3.11}$$

If we express the velocity in terms of temperature in (3.11) and use (3.10), we obtain

$$\frac{n^3(n^2-l^2)}{Z_1^4}\left(\frac{\Delta E}{kT}\right)^2 \ll \frac{n^2}{n_0}\sqrt{\theta}\,\frac{\Delta E}{kT} \ll 1. \tag{3.12}$$

Since, according to (2.3), $\Delta E/kT \ll 1$, the condition for the validity of the Born approximation is satisfied provided that n is not too large.

B. Cross section and transition rates for ion-ion collisions

As already noted, Coulomb repulsion between the colliding ions must be taken into account in calculations of transition probabilities for ion-ion collisions or, in other words, the actual hyperbolic paths must be used for the relative motion of the ions. However, it turns out that, in contrast to the case of electron-ion collisions, the cross sections for a broad class of transitions can be calculated by using the simple approximation given by (3.5) for the inelastic interaction potential.

In fact, if the relative velocity of the ions is not too high, i.e.,

$$v \ll \sqrt{\frac{Z_1 Z_2}{R_0 M}} \quad \text{and} \quad \theta \ll \frac{2n_0^2 Z_1}{Z_2 R_0} \tag{3.13}$$

(this is practically always valid for collisions between multiply-charged ions), the Coulomb repulsion ensures that the separation R between them is always greater than R_0 even for collisions with zero impact parameter, so that the true inelastic interaction potential can be replaced by (3.4). The cross section for the transition in first-order perturbation theory is

$$\sigma_{12}(v) = 8\pi\left(\frac{\lambda}{v}\right)^2 e^{-\nu\pi}\left[-\nu K_{i\nu}(\nu) K'_{i\nu}(\nu)\right] = 8\pi\left(\frac{\lambda}{v}\right)^2 \Phi(\nu), \tag{3.14}$$

where $K_{i\nu}(\nu)$ is the Macdonald function with imaginary index and the function $\Phi(\nu)$ is tabulated in Ref. 67 and has the following asymptotic behavior:

$$\Phi(\nu) = \begin{cases} \ln\dfrac{2}{\gamma\nu}, & \gamma = e^C = 1.781\ldots, \quad \nu \to 0, \\ \dfrac{\pi}{\sqrt{3}}\exp(-2\pi\nu), & \nu \to \infty. \end{cases} \tag{3.15}$$

Averaging of $v\sigma_{12}(v)$ over the Maxwellian distribution for ions with temperature T_i yields

$$\langle v\sigma_{12}\rangle = \frac{\lambda^2}{v_T}\Psi(\xi), \tag{3.16}$$

where

$$v_T = \sqrt{\frac{T_i}{M}}, \quad \xi = \frac{Z_1 Z_2 \omega}{M v_T^3},$$

$$\Psi(\xi) = 8\sqrt{2\pi}\int_0^\infty x\exp\left(-\frac{x^2}{2}\right)\Phi\left(\frac{\xi}{x^3}\right)dx$$

$$= \begin{cases} 20\ln(1.39/\xi), & \xi \to 0, \\ 73.2\,\xi^{0.2}\exp(-2.7\xi^{0.4}), & \xi \to \infty. \end{cases}$$

It is important to emphasize that (3.14) and (3.16) were derived in first-order perturbation theory, i.e. in the Born approximation. However, for ion-ion collisions, the condition for the validity of this approximation is frequently not satisfied, and this leads to the violation of the unitarity of the scattering matrix, so that the transition probability $W_{12}(\rho, v)$, calculated in first-order perturbation theory, may turn out to be greater than unity for a certain range of values of the parameters ρ, v, ω, and λ. The cross sections and excitation rates calculated from (3.14) and (3.16) are then generally too high. To remove this defect, we can use the normalization procedure which is reasonably well tested in the theory of atomic collisions.[64,73] In particular, we restrict the transition probability by setting

$$W_{12}^{\mathrm{H}}(\rho, v) = \min\left\{\frac{1}{2}, W_{12}(\rho, v)\right\}, \tag{3.17}$$

where $W_{12}(\rho, v)$ is given by the formulas of the Born approximation. It can then be readily shown that the normalized cross sections and transition rates can be written in the form[75,76]

$$\sigma_{12}^{\mathrm{H}}(v) = \left(\frac{\lambda}{v}\right)^2\beta(v, \eta), \quad \langle v\sigma_{12}^{\mathrm{H}}\rangle = \frac{\lambda^2}{v_T}E(\xi, \eta), \tag{3.18}$$

where $\eta = M\lambda\sqrt{\lambda\omega}/Z_1Z_2$, and β, E are certain universal functions. Graphs of β and E, obtained by numerical calculations on a computer,[75] are shown in Figs. 7–8. These results can readily be used to determine the cross sections and excitation rates for a broad range of transitions occurring during ion-ion collisions. For example, Fig. 9 shows the rates for the reactions

$$\mathrm{MgXII}\,(2s_{1/2}) + \mathrm{Mg}^{+12} \to \mathrm{MgXII}\,(2p_{1/2}) + \mathrm{Mg}^{+12},$$
$$\mathrm{MgXII}\,(2s_{1/2}) + \mathrm{Mg}^{+12} \to \mathrm{MgXII}\,(2p_{3/2}) + \mathrm{Mg}^{+12},$$

calculated with the aid of Fig. 8, and the rates for these transitions during electron-ion collisions, calculated from (2.7). We note that it is clear from Fig. 9 that the ion excitation rate may substantially exceed the electron rate for transitions with various small resonance defects (the transition $2s_{1/2} \to 2p_{1/2}$). Further details can be found in Ref. 77 and in the next Section of this review.

C. Influence of plasma polarization effects on the frequency of inelastic collisions

The exceedingly high plasma density reached in iner-

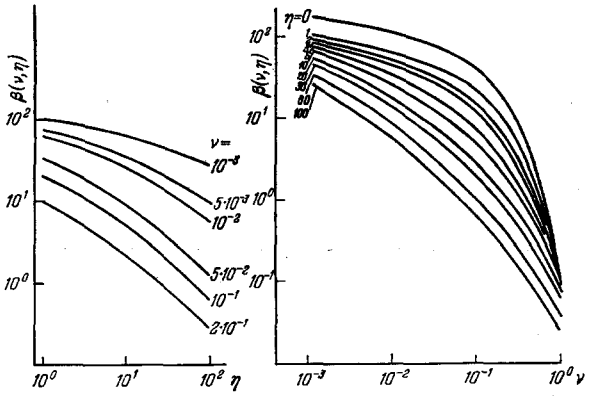

FIG. 7. Plots of $\beta(\nu,\eta)$, which determine the cross sections for inelastic transitions during ion-ion collisions.

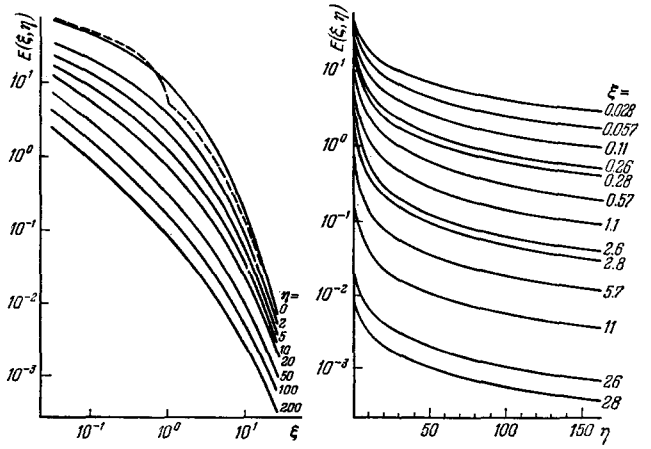

FIG. 8. Plots of $E(\xi,\eta)$, which determine the rate of inelastic transitions during ion–ion collisions. Broken curve shows the asymptotic behavior of the function $E(\xi,0)$ [see (3.16)].

tial confinement systems leads us to the consideration of the influence of polarization effects on excitation processes during inelastic collisions. In fact, charged plasma particles in the first place screen the field due to the exciting particle and, next, as the particle flies past an atom, it induces a variable dipole moment in the plasma which, in general, will have a Fourier component at the frequency of the atomic transition. The spectroscopic consequences of these effects have been examined in the literature in connection with the emission of forbidden lines,[78,79] and the theory of spectral line broadening.[80] The effect of Debye screening in dense plasmas on recombination coefficients and the broadening of Lyman lines have also been discussed.[81–83] In actual fact, polarization effects do not reduce to Debye screening. If the excitation energy $\hbar\omega_{12}$ of the atomic transition is of the order of $\hbar\omega_L$ (where ω_L is the Langmuir frequency), it is found that the frequency dispersion of the plasma permittivity becomes important.[84,85] This must be borne in mind in the case of collisional transitions between highly excited states and between fine structure components.

The influence of plasma effects on the inelastic transition frequency is conveniently described not within the framework of collision theory but by considering the atom or ion placed in the random field $V(r,t)$ due to the entire ensemble of charged particles in the plasma. The probability of the inelastic $1\to 2$ transition in first-order perturbation theory is then given by[85]

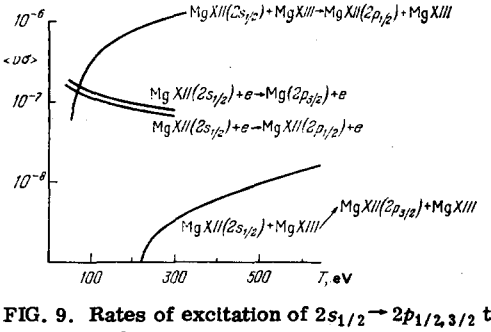

FIG. 9. Rates of excitation of $2s_{1/2}\to 2p_{1/2,3/2}$ transitions by electron and ion impact.

$$\nu_{12}=2\pi\int |A(q)|^2 V^2(q,\omega_{12})\,dq, \tag{3.19}$$

where $V^2(q,\omega_{12})$ is the spectral density of fluctuations in the potential $V(r,t)$, the atomic formfactor is given by

$$A(q)=\int \psi_1(r)\,\psi_2^*(r)\,e^{iqr}\,dr, \tag{3.20}$$

and $\psi(r)$ are the atomic wave functions. Polarization effects can readily be included in the spectral density $V^2(q,\omega_{12})$ of the fluctuations when the transition probability is given in the general form (3.19). In the limiting case of tenuous plasma, when the frequency of inelastic collisions obviously reduces to the product $N_i\langle v\sigma_{12}\rangle$ (σ_{12} is the excitation cross section), the expression given by (3.19) corresponds to the spectral density of fluctuations in the ideal electron gas.

If we use (3.20) for the atomic formfactor, we can write the inelastic collision frequency for closely spaced levels in the form

$$\nu_{12}=\frac{N_e 8\sqrt{2\pi}\lambda^2 f(\alpha,\beta)}{(\omega R_0)},$$
$$f(\alpha,\beta)=\frac{R_0^2}{\alpha}\int_0^\infty q\,dq K_1^2(qR_0)\,|\varepsilon(q,\omega_{12})|^{-2}\exp\left(-\frac{\omega_{12}^2}{2q^2v_T^2}\right), \tag{3.21}$$

where K_1 is the Macdonald function, the longitudinal permittivity of the plasma is given by

$$\varepsilon(q,\omega)=1-\beta\Phi(x)+\frac{i\beta}{x}\sqrt{\frac{\pi}{2}}\exp\left(-\frac{1}{2x^2}\right),$$

where $\beta=(\omega_L/\omega_{12})x=qv_T/\omega_{12}$, and $\Phi(x)$ is the plasma dispersion function.[86] When $\beta=0$, the function $f(\beta,\beta)$ becomes identical with $f(\alpha)$ [see (3.7)] and, when $\beta\neq 0$, the function $f(\alpha,\beta)$ represents the plasma polarization effect (see Fig. 6). We conclude that polarization effects are important if the plasma frequency is comparable with the atomic transition frequency, and the Debye length is comparable with the characteristic length for the atomic interaction.

4. RELATIVE SPECTRAL-LINE INTENSITIES OF MULTIPLY-CHARGED IONS IN DENSE PLASMA

A. Intensity ratio for the fine-structure components of a resonance line of hydrogen-like ions

Consider the elementary processes that govern the intensity of the Lyman doublet of hydrogen-like ions. Even this apparently simple spectrum gives an intensity ratio that is a function of density. The point to note first is that, in this case, the coronal and Boltzmann limits of the intensity ratio of the fine-structure components, i.e., $\beta=I(2p_{1/2}\to 1s_{1/2})/I(2p_{3/2}\to 1s_{1/2})$ (Fig. 10) are equal: $\beta_C=\beta_B=1/2$. This is so because the radiative decay probabilities for the $2p_{1/2}$ and $2p_{3/2}$ sublevels are equal, and their rates of population by electron impact from $n\neq 2$ levels (including the continuum) are proportional to the statistical weights. However, for intermediate electron densities, when neither the coronal nor the Boltzmann models are valid, we have $\beta\neq 1/2$, so that we have to consider the balance equations for the $2s_{1/2}$, $2p_{1/2}$, and $2p_{3/2}$ level populations (represented by subscripts 1, 2, and 3, below):[77]

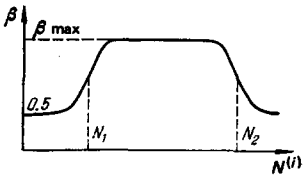

FIG. 10. Ratio β of the intensities of the fine-structure components of the L_α line emitted by a hydrogen-like ion as a function of plasma density.

$$\begin{cases} N_1[A_1+N^{(i)}(C_{12}+C_{13})]=q_1+N_2N^{(i)}C_{21}+N_3N^{(i)}C_{31}, \\ N_2[A_2+N^{(i)}(C_{21}+C_{23})]=q_2+N_1N^{(i)}C_{12}+N_3N^{(i)}C_{32}, \\ N_3[A_3+N^{(i)}(C_{31}+C_{32})]=q_3+N_1N^{(i)}C_{13}+N_2N^{(i)}C_{23}, \end{cases} \quad (4.1)$$

where $N^{(i)}C^i_{jk}=N^{(i)}(C^e_{jk}+1/\xi C^e_{jk})$, $\xi=N^{(i)}/N_e$; $N^{(i)}$ is the density of the ions, q_j is the rate of population of the j-th level by electron impact from states with $n\neq 2$, A_j is the probability of radiative decay of the j-th level to the ground state $1s_{1/2}$, and C_{jk} are the resultant rate coefficients describing transitions between fine-structure sublevels due to ion-ion and electron-ion collisions.

The following simplifying assumptions can be used to solve (4.1): (1) the rate of the $2p_{1/2} \rightleftarrows 2p_{3/2}$ quadrupole transition is much less than the rates of the optically allowed $2s_{1/2} \rightleftarrows 2p_{1/2}$ and $2s_{1/2} \rightleftarrows 2p_{3/2}$ transitions (i.e., $C_{23} \ll C_{12}, C_{13}$); (2) the radiative decay of the $2s_{1/2}$ level, connected with the two-photon transition, and its probability are practically always found to satisfy the condition[87] $A_1 \ll A_2 = A_3$, and (3) fine splitting does not exceed a few electron volts, which is usually much less than the electron temperature of the plasma, so that the probability of direct and reverse transitions $1 \rightleftarrows 2$ and $1 \rightleftarrows 3$ and the pumping rates q_2 and q_3 are proportional to the statistical weight of the final state, i.e., $C_{31} = \frac{1}{2}C_{13}$, $C_{21}=C_{12}$, and $q_2=\frac{1}{2}q_3$. Solution of (4.1) under these assumptions yields the following expression for the intensity ratio for the fine-structure components:[77]

$$\beta=\frac{1}{2}\left\{1+\frac{3(q_s/q)[\alpha-(1/3)]N^{(i)}/N_0}{\frac{2A_1C_{\min}q_p}{3A_2C_{\max}q}+\left[\frac{2}{3}-\frac{q_s}{q}\left(\alpha-\frac{1}{3}\right)\right]\frac{N^{(i)}}{N_0}+\left(\frac{N^{(i)}}{N_0}\right)^2}\right\}, \quad (4.2)$$

where $q_s=q_1$, $q_p=q_2+q_3$, $q=q_s+q_p$, $C_{\max}=C_{12}+C_{13}$, $C_{\min}=C_{12}C_{13}/C_{\max}$, $\alpha=C_{12}/C_{\max}$, and $N_0=A_2/C_{\min}$.

It is clear from (4.2) that, if $\alpha\neq 1/3$, i.e., the ratio of the $2s_{1/2}\rightarrow 2p_{1/2}$ and $2s_{1/2}\rightarrow 2p_{3/2}$ transition probabilities does not correspond to the ratio of the statistical weights of the $2p_{1/2}$ and $2p_{3/2}$ levels, the quantity β is a function of the plasma temperature and density. The dependence of β on $N^{(i)}$ can then be characterized as follows.

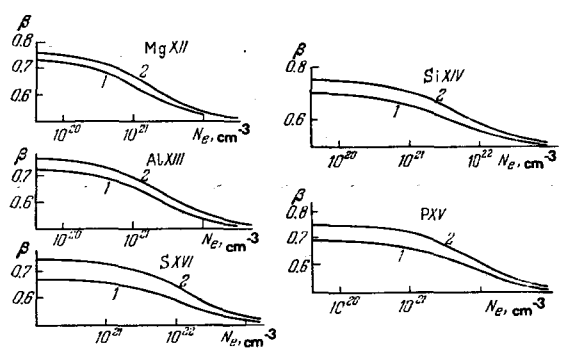

FIG. 11. Plots of $\beta(N_e)$ for MgXII–SXVI with $\theta_e=\theta_i=0.1$ (curve 1) and $\theta_e=\theta_i=0.3$ (curve 2) in the range $N_e\sim 10^{20}$–10^{22} cm^{-3}.

At low and high densities, which correspond to the coronal and Boltzmann distributions, respectively, the quantity β does not depend on the plasma parameters and is equal to the ratio of the statistical weights of the $2p_{1/2}$ and $2p_{3/2}$ levels, i.e., 1/2. In the intermediate region, $N_1 \ll N^{(i)} \ll N_2$ (where $N_1=A_1/C_{\max}$, $N_2=N_0$), the quantity β is practically a constant and is determined by the ratio of pumping rates to the $2s$ and $2p$ states and the rates of mixing of these levels:

$$\beta=\beta_{\max}=\frac{1}{2}\left[1+\frac{3(q_s/q)\left(\alpha-\frac{1}{3}\right)}{(2/3)-(q_s/q)\left(\alpha-\frac{1}{3}\right)}\right]. \quad (4.3)$$

Moreover, there are the two intermediate regions $N^{(i)}\sim N_1$ and $N^{(i)}\sim N_2$ in which β varies from 1/2 to $\beta_{\max}$ (see Fig. 10).

The results given in Sec. 3 in connection with the transition rates between closely lying levels in the case of electron-ion and ion-ion collisions can readily be used to calculate C_{jk} and hence, using (4.2), to construct β as a function of N_e for plasmas with different charge compositions. For ions with nuclear charges $Z=12$–16, the quantities N_1 and N_2 amount to 10^{13}–10^{15} and 10^{19}–10^{21} cm^{-3}, respectively. Hence, it follows that, whereas the first intermediate region is of interest for the diagnostics of tenuous astrophysical plasmas and plasmas in tokamaks, the function $\beta(N_e)$ in the second intermediate region can be used for the diagnostics of dense laboratory plasmas (laser plasmas, plasmas heated by relativistic electron beams, and so on). Figure 11 shows β as a function of the plasma density in the second intermediate region for ions with $Z=12$–16 and different values of the electron temperature $\theta_e=\theta_i=kT_e/Z^2\mathrm{Ry}$.

It is clear from (4.3) that the maximum value of β is determined by the rates of population of the $2s$ and $2p$ states. In particular, in the example shown in Fig. 11, this ratio is determined by the rates of excitation of the $2s$ and $2p$ states by electron impact from the ground state, which corresponds to the case of stationary plasma. In a cooling plasma, the recombinational population mechanism is possible in principle and leads to a different value of $\beta_{\max}$. In particular, $\beta\gtrsim 2$ becomes possible (see Ref. 77 for further details).

It is important to emphasize that (4.2) can be used only in the case of optically thin plasmas, i.e., in the absence of resonance radiation trapping. In practice, at least in the case of inertial confinement, this means that diagnostics must rely on the ions of elements introduced as impurities into the target. This type of experiment has been carried out.[88]

B. Intensity ratio for resonance and intercombinational lines of helium-like ions

For helium-like ions with $Z<20$, the probability of radiative decay of the 2^3P_1 triplet state is lower by

several orders as compared with the corresponding probability for the 2^1P_1 singlet state, whereas the excitation cross sections are roughly equal (the level scheme is shown in Fig. 12). This means that the coronal and Boltzmann values of the intensity ratio are also different by several orders (see Fig. 5). In the intermediate region, where the rate of collisional de-excitation of the 2^3P state becomes larger than the rate of its radiative decay, the population of the 2^3P state will be proportional to the density of ions in the ground state, N_0. At the same time, the population of the 2^1P_1 state will be proportional to the product $N_0 N_e$, as in the case of very low densities. Thus, the intensity ratio for the $2^1P_1 \to 1^1S_0$ resonance line and the $2^3P_1 \to 1^1S_0$ intercombination line turns out to be proportional to the plasma density N_e and is very convenient for the determination of this density.

This method was first used in studies of the θ-pinch plasmas.[89] It has also been used to determine the density of laser plasmas.[90] The next step was to investigate the influence of different elementary processes such as cascade excitation and three-particle and photo-recombination.[91] Vaĭnshteĭn[92] has pointed out that exchange has to be taken into account in calculations of the cross sections for the excitation of singlet states, and this has removed the serious discrepancy between experimental (astrophysical) and theoretical values of relative intensities at low densities. Detailed calculations have been carried out[91] for a broad range of plasma parameters, taking into account all the collisional and radiative processes for levels with principal quantum number $n \leq 4$. Figure 13 shows numerical calculations of the ratio $\alpha = I(2^1P_1 \to 1^1S_0)/I(2^3P_1 \to 1^1S_0)$ for the ion MgXI at $kT_e = 250$ eV. The shape of the $\alpha(N_e)$ curve is determined by different processes in different regions.

For $N_e < 10^{11}$ cm^{-3}, the ratio α is independent of N_e. The probabilities of radiative decay of all the levels, including 2^3S_1, 2^1S_0, 2^3P_0, and 2^3P_2, are then higher than their rates of collisional de-excitation. For N_e between 10^{11} and approximately 10^{16} cm^{-3}, the probabilities of radiative decay of the "metastable" 2^3S_1, 2^3P_0, and 2^3P_2 levels become successively lower than the probabilities of collisional transitions between the triplet states. (We note, by the way, that the rates of collisional transition between triplets and singlets are lower by one or two orders of magnitude than the rates of transition between levels of the same multipolarity). Hence, all the triplet states begin to emit as a result of the $2^3P_1 \to 1^1S_0$ transition. For 10^{16} cm$^{-3} < N_e < 10^{19}$ cm^{-3}, the ratio α is again density-independent and is

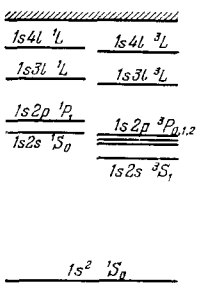

FIG. 12. The lower excited states of a helium-like ion.

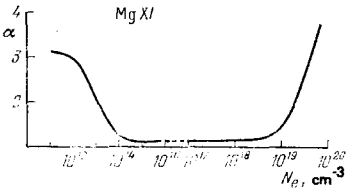

FIG. 13. Intensity ratio α for the resonance and intercombinational lines of the helium-like ion MgXI as a function of plasma density.

determined by the ratio of the total rates of excitation of the group of singlets (2^1S_0 and 2^1P_1) and the group of triplets (2^3S_1 and $2^3P_{0,1,2}$).

For $N_e > 10^{19}$ cm^{-3}, the probability of collisional transitions from the 2^3S and 2^3P levels to the singlet level 2^1L and the probability of their ionization become greater than the probability of radiative decay $A(2^3P_1 \to 1^1S_0)$. The ratio α is then proportional to N_e.

Next, for $N_e \gtrsim 10^{22}$ cm^{-3} collisional de-excitation processes become appreciable for the 2^1P_1 level as well and, when Boltzmann equilibrium is reached, α becomes equal to the ratio of the radiative transition probabilities (~ 1000).

Calculations of level populations for helium-like ions have been reported for a broad range of densities.[91,93-95] Figures 14–16 show the function $\alpha(N_e)$ deduced from these data for the ions NaX-ArXVII in the region $N_e \sim 10^{19}$–10^{23} cm^{-3}, which is particularly interesting from the point of view of plasma diagnostics. The very unexpected result is that the density of the upper intercombinational line $3^3P_1 \to 1^1S_0$, first observed by Boiko *et al.*,[95] has turned out to be a function of density. The intensity ratio ε for the allowed ($3^1P_1 \to 1^1S_0$) and the intercombinational ($3^3P_1 \to 1^1S_0$) lines measured in Ref. 95 is much greater than predicted by both the coronal and Boltzmann models. It has turned out that the anomalously high intensity of the line is due to the cascade population of triplet levels.

In fact, at low densities, which correspond to the coronal distribution, the ratio ε is independent of N_e and its magnitude is equal to the coronal value (~ 50 in the case of MgXII). Higher plasma densities lead to an increase in the relative population of the 3^3P level through cascade excitation of this state via the meta-

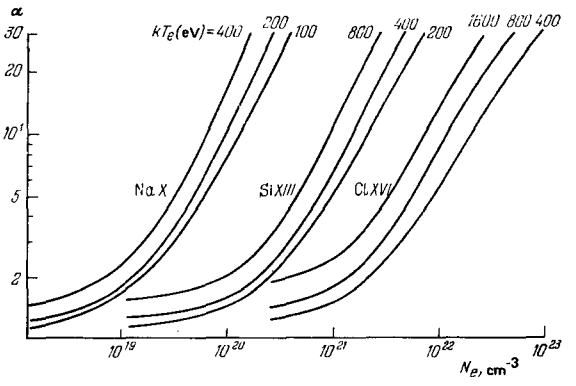

FIG. 14. Plots of $\alpha(N_e)$ for NaX, SiXIII, and ClXVI at different plasma temperatures.

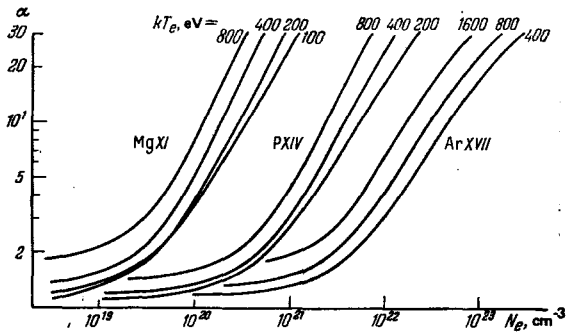

FIG. 15. Same as Fig. 14, for MgXI, PXIV, and ArXVII.

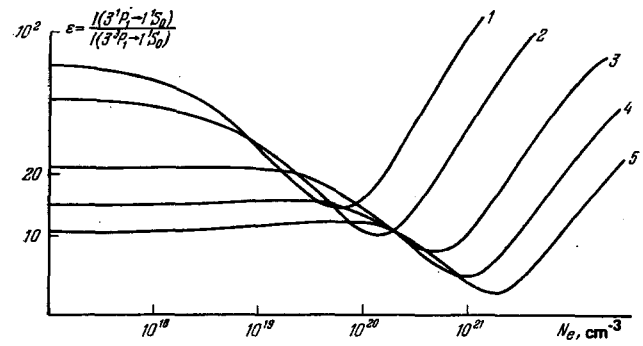

FIG. 17. Ratio $\varepsilon = I(3^1P_1 \to 1^1S_0)/I(3^3P_1 \to 1^1S_0)$ as a function of electron density in plasma: 1—MgXI, $kT_e = 172$ eV; 2—AlXII, $kT_e = 172$ eV; 3—PXIV, $kT_e = 345$ eV; 4—SXV, $kT_e = 345$ eV; 5—ClXVI, $kT_e = 345$ eV.

stable triplet state 2^3L, and the ratio ε decreases. Further increase in the density ensures that collisional intercombinational transitions between the 2^3L and 2^1L levels begin to reduce the population of the 2^3L level and, consequently, of the 3^3P level as well. The ratio ε then begins to increase, tending to its Boltzmann value (approximately 500 in the case of MgXI; see Fig. 17).

There is thus a relatively narrow range of values of the plasma density ($N_e \approx 10^{20}$–10^{21} cm^{-3} for ions with $Z \approx 11$–14) in which the allowed ($3^1P_1 \to 1^1S_0$) and intercombinational ($3^3P_1 \to 1^1S_0$) lines have similar intensities. The fact that the laser plasma investigated in Ref. 95 had an electron density N_e corresponding precisely to this region was indeed responsible for a detectable $3^3P_1 \to 1^1S_0$ line. The detection of this line in laser plasma and the detection of the $2^3P_1 \to 1^1S_0$ line have resulted in quantitative data on plasma electron density (Fig. 17). Moreover, the high intensity of the $3^3P_1 \to 1^1S_0$ lines confirms the cascade mechanism as the origin for the population inversion through the intercombinational transitions $1s3^3L \to 1s2^1L'$,[93,94] whose wavelengths lie in the x-ray band.

C. Intensity ratio for dielectronic satellites of a resonance line of hydrogen-like ions

Dielectronic satellites arise in the x-ray spectra of multiply-charged ions as a result of transitions from doubly excited states of ions with the preceding degree of ionization. Satellites in the spectra of hydrogen-like ions with $Z \gtrsim 10$ are readily recorded, as are the resonance lines themselves. Satellite line intensities are

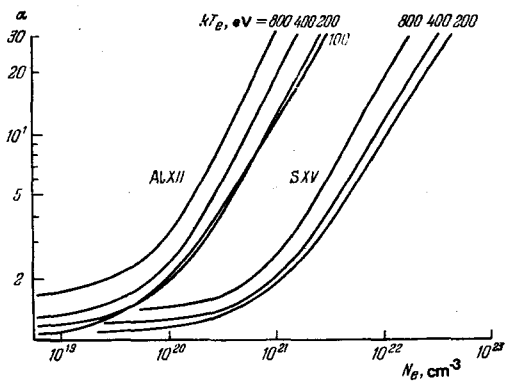

FIG. 16. Same as Figs. 14 and 15, for AlXII and SXV.

usually interpreted in terms of the coronal model for population[46,47] on the basis of relativistic calculations of radiative (A) and radiationless (Γ) de-excitation of levels beyond the continuous spectrum limit. The use of this model is justifiable only for tenuous astrophysical plasmas where collisional transitions between doubly-excited levels of helium-like ions are unimportant. In the coronal model, the satellite intensity I increases with increasing autoionization probability Γ:

$$I = \frac{g}{g_1} 4\pi^{3/2} a_0^3 N_e N_H(1s) \left(\frac{\mathrm{Ry}}{kT_e}\right)^{3/2} \exp\left(-\frac{E}{kT_e}\right) \frac{A\Gamma}{\Gamma + \Sigma A}; \qquad (4.4)$$

where $N_H(1s)$ is the density of the hydrogen-like ions in the ground state, $g_1 = 2$ is the statistical weight of the ground state, a_0 is the Bohr radius, g is the statistical weight of the autoionization state, and E is its energy measured from the ionization limit of the He-like ion.

Values of Γ may differ by a factor of up to 100 for different satellites.[57] It then follows from the coronal model (4.4) that, when $A \gtrsim \Gamma$, the satellite intensities should also differ by an analogous factor. However, the spectroscopy of plasmas produced by neodymium and iodine laser beams under different irradiation conditions and for different parameters of the heating radiation[96] has shown that satellites with low Γ are much stronger than predicted by the coronal model. It has been shown[97] that the reason for this discrepancy is the departure of dense plasmas from the coronal model. Indeed, the doubly-excited states in dense plasmas are populated not only through dielectronic capture but also through collisional transitions from near-lying autoionization states. As a result, the intensity ratio of a number of satellite lines depends on N_e and can be used to determine the electron density of the plasma. The advantage of this particular diagnostic method is that radiation-trapping effects which, in general, distort the intensity and the shape of the resonance lines themselves, are unimportant for satellites because the lower levels for the satellites are the excited states of the helium-like ions.

The populations of doubly-excited levels of helium-like ions and, consequently, the intensities of the satellite lines, must be determined by solving the balance equation (see Fig. 18 for the level scheme)

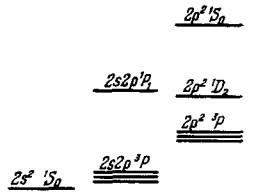

FIG. 18. Doubly excited levels of a helium-like ion.

$$N_i(\Gamma_i + A_i + \sum_{k\neq i} N_e C_{ik}) = Q_i N_{\rm H}(1s) + \sum_{k\neq i} N_k N_e C_{ki}, \qquad (4.5)$$

where Q_i is the probability of dielectronic capture to the i-th level.

When (4.5) is solved, it must be remembered that satellites of the lines of hydrogen-like ions are strong only if the concentration of the hydrogen-like ions is high enough, i.e., usually for $kT_e \gtrsim Z^2$Ry. The rates of collisional transitions within the singlet and triplet systems at such temperatures are much greater than the rate C_{Ts} of transitions between triplets and singlets.[58] Hence, when $N_e \ll N_0 = (A+\Gamma)/C_{Ts}$, the balance equations for the triplet and singlet level schemes can be considered separately. The triplet level populations have been calculated[97] with a view to determining the intensity ratio for the two groups of satellite lines

1) $2s2p\ {}^3P_2 \to 1s2s\ {}^3S_1$, $2s2p\ {}^3P_1 \to 1s2s\ {}^3S_1$, $2s2p\ {}^3P_0 \to 1s2s\ {}^3S_1$;
2) $2p^2\ {}^3P_2 \to 1s2p\ {}^3P_2$, $2p^2\ {}^3P_2 \to 1s2p\ {}^3P_1$, $2p^2\ {}^3P_1 \to 1s2p\ {}^3P_1$, $2p^2\ {}^3P_1 \to 1s2p\ {}^3P_0$.

The analytic expressions obtained in Ref. 97 have resulted in a dependence of the intensity ratio for these two groups of lines $\kappa = I_2/I_1$ on the plasma density which can be qualitatively described as follows.

At low densities (coronal limit), dielectronic capture gives rise to a preferential population of the $2s2p^3P$ level, whereas the population of the $2p^2\ {}^3P$ levels is low. As the density increases, the $2p^2\ {}^3P$ levels are mainly populated by excitation from the $2s2p^3P$ levels and the ratio κ increases. At still higher densities (collisional transitions), the Boltzmann distribution is established within the triplet system. The important point is that the Boltzmann equilibrium between the triplet levels is established even for $N_e \ll N_0 = (A+\Gamma)/C_{Ts}$ because the rate of collisional $2s2p^3P \rightleftarrows 2p^2\ {}^3P$ transitions is greater by roughly two orders of magnitude as compared with the rate of intercombinational transitions (C_{Ts}).

Figure 19 shows the calculated intensity ratios for the above two groups of satellite lines in the range $N_e \sim 10^{20}$–10^{23} cm^{-23}.

D. Intensity ratio for lines of oxygen-like ions

The spectra of ions with the $2s^22p^k$ ($k=1$–6) electronic configuration in the 70–200 Å band have been extensively investigated in recent years.[98,99] Moreover, it has been pointed out[100] that the electron density can be determined from the relative rates of transition between levels with principal quantum number $n=2$ in this wavelength band. This method is very important for two reasons.

First, it can be used to extend the range of the diagnosed plasma parameters, both in density and in

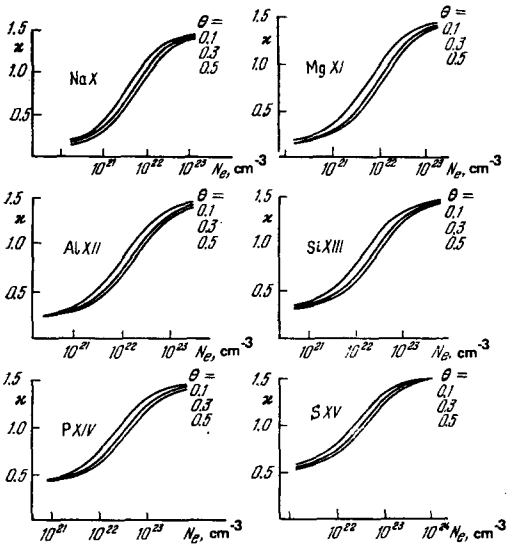

FIG. 19. Intensity ratio κ of satellite lines of NaX–SXV as a function of plasma density.

temperature, when it is employed in conjunction with diagnostic methods based on relative intensities of lines due to hydrogen- and helium-like ions and their satellites.

Second, plasmas containing multiply-charged ions with the $2s^22p^k$ configuration are currently regarded as promising media for lasers operating in the far ultraviolet.[101–107,22] It turns out that the amplification coefficient that can be achieved for a given transition has a well-defined maximum as a function of electron density.[104] In view of this, it is very desirable to develop methods for density diagnostics based on the spectra of ions with the $2s^22p^k$ configuration as a way of optimizing the lasing conditions.

We shall now follow the method used in Ref. 108 to consider processes that govern the populations of excited states of oxygen-like ions with principal quantum numbers $n=2$ (the level scheme is shown in Fig. 20).

Estimates of the cross sections for collisional transitions show that the main contribution to the relaxation constants is provided by electron-ion collisions. The occupation of levels belonging to the $2s2p^5$ configuration occurs during excitation by electron impact from the $2s^22p^4$ configuration. Excitation of the $2p^6\ {}^1S_0$ level from the ground state corresponds to a dielectronic transition, the cross section for which is very low (much less than the cross section for the excitation of the one-electron transition[109]), so that the population of this level in dense plasma takes place with much higher efficiency.

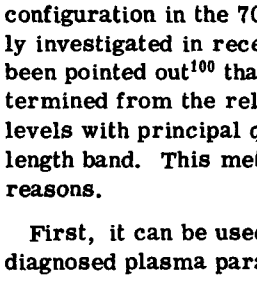

FIG. 20. Level scheme for the lower excited states of an oxygen-like ion.

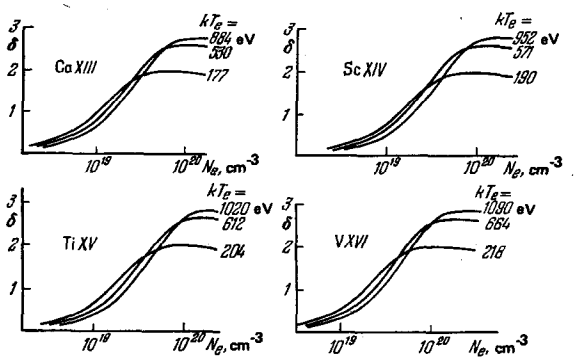

FIG. 21. Intensity ratio δ for the lines of oxygen-like ions CaXIII, ScXIV, TiXV, and VXVI as a function of the electron density of plasma.

through the cascade transition via the $2s2p^5\,^1P_1$ state. The decay of the $2s2p^5$ level occurs during radiative and collisional transitions to levels of the ground-state configuration. The $2p^6\,^1S_0$ level decays through transitions to $2s2p^5$ levels.

The solution of the kinetic equations for the populations of the above levels with allowance for the above processes can readily be obtained analytically.[108] The solution has been used[110] to calculate the intensity ratio $\delta = I(2p^6\,^1S_0 \rightarrow 2s2p^5\,^1P_1)/I(2s2p^5\,^3P_2 \rightarrow 2s^22p^4\,^3P_1)$ for oxygen-like ions CaXIII-FeXIX as a function of the plasma density (see Figs. 21–22). It is clear from these figures that the temperature dependence of δ is very weak. This is very convenient from the point of view of electron density determinations. This method has been used[108] to determine the density of laser plasmas from the spectra of the ions CaXIII and TiXV.

5. SPECTROSCOPIC DIAGNOSTICS OF SUPERDENSE PLASMAS

The method discussed in Sec. 4 of this review can be used to determine the electron density of plasmas in the range $N_e \sim 10^{19}$–10^{23} cm^{-3} from the relative intensities of x-ray lines of ions with $Z \sim 10$–15 (see Figs. 11, 14–17, 19, 21, 22). In principle, these methods can also be used for $N_e \gtrsim 10^{23}$ cm^{-3} when the ion charge is greater. However, the plasma must then contain ions with very high ionization potentials ($I_i \gtrsim 3.5$ keV), which

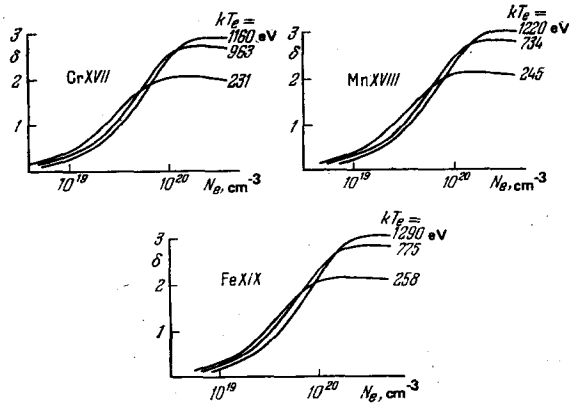

FIG. 22. Same as in Fig. 21, for the ions CrXVII, MnXVIII, and FeXIX.

are excited only at very high temperatures. It is, therefore, very desirable to reach the high-density region not as a result of an increase in the charge of the ion, but through a suitable choice of the spectral lines of ions with given Z. In other words, it will be interesting to consider the difference between the actual distribution over the excited states for an ion with fixed Z and the Boltzmann distribution as the plasma density increases. To solve this problem, we return to (2.1), which is the condition for the establishment of the Boltzmann distribution between the two levels 1 and 2. It is clear from this condition that, as the electron density increases, the Boltzmann equilibrium is eventually established between levels satisfying the following two conditions: (a) the probabilities of radiative decay of both levels are high (i.e., radiative decay is determined by optically allowed transitions), and (b) the rate of collisional transitions between the levels is relatively low (for example, between levels with different multiplicity). It is readily seen that the cases examined in Sec. 4 do not satisfy both these conditions at the same time. In fact, for the triple 2^3P state (Sec. 4b), condition (a) is not satisfied because the decay of these states is determined by the weak spin-orbit interaction and the radiative decay probability A is low. In the other cases (Secs. 4a, c–d), condition (a) is satisfied, but the levels are connected by dipole collisional transitions, the rate of which is high [condition (b) is not satisfied].

Conditions (a) and (b) can be satisfied simultaneously for triplet and singlet doubly excited states of helium-like ions. In fact, the radiative decay of such states corresponds to a strong resonance transition [condition (a) is satisfied] and the rate of collisional transitions is low because these levels have different multiplicities [condition (b) is satisfied]. In view of the foregoing, the establishment of the Boltzmann distribution and the change in the relative intensities of the spectral lines in this system occur at much higher densities as compared with the cases considered above. This system is therefore the most promising from the point of view of superdense plasma diagnostics.[111]

Let us now consider the change in the relative populations of doubly-excited states of helium-like ions during a transition from tenuous to dense plasma (Fig. 18 shows the energy levels). We note, to begin with, that the establishment of the Boltzmann distribution between the levels occurs in two stages. First, when $N_e \sim A/C$, where C is the rate of collisional transitions of the triplet-triplet or singlet-singlet type, the Boltzmann distribution is established separately in the triplet and singlet system. This range of values of N_e was discussed in detail in Sec. 4c. As the density increases up to $N_e \sim A/C_{TS}$, where C_{TS} is the rate of collisional transitions between the triplet and the singlet levels, the Boltzmann distribution begins to set in between states with different multiplicity as well, and this again leads to a change in the intensity ratio for certain lines.

The relative populations of singlet and triplet states can readily be determined in this region from the balance equations for the system of levels shown in Fig.

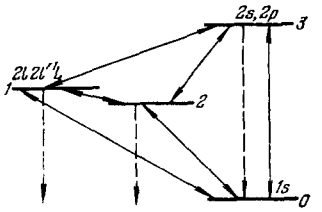

FIG. 23. Scheme used in the calculation of the intensity ratio σ for triplet and singlet satellites in superdense plasma (the central level is $2l2l'^3L$).

23:

$$\left.\begin{aligned} N_1(A_1+\Gamma_1+W_{12}+W_{13}) &= N_0Q_{01}+N_2W_{21}+N_3W_{31},\\ N_2(A_2+\Gamma_2+W_{21}+W_{23}) &= N_0Q_{02}+N_1W_{12}+N_3W_{32},\\ N_3(A_{30}+W_{30}+W_{32}) &= N_0Q_{03}+N_1W_{13}+N_2W_{23} \end{aligned}\right\} \qquad (5.1)$$

where subscripts 1, 2, 3, and 0 represent, respectively, the systems of singlet and triplet doubly-excited levels of the helium-like ion, levels with $n=2$, and the ground state of the hydrogen-like ion. The equations given by (5.1) thus include autoionization and radiative decay, dielectronic capture, ionization, ternary recombination, and collisional intercombinational transitions. Solution of (5.1) yields the following expression for the ratio of populations of triplet and singlet levels:

$$\frac{N_2}{N_1}=D_1\frac{1+D_3N_e+D_5N_e^2+D_6N_e^3}{1+D_4N_e+D_6N_e^2+D_7N_e^3}, \qquad (5.2)$$

where:

$$D_1=\frac{g_2q_{02}(A_1+\Gamma_1)}{q_1q_{01}(A_2+\Gamma_2)},\quad D_2=\frac{C_{30}}{A_{30}}+\frac{C_1+(q_{01}C_{21}/q_{02})}{A_1+\Gamma_1},$$
$$D_3=\frac{b}{A_{30}S}\left(\frac{C_2}{g_2}+\frac{q_{03}}{q_{02}}C_i\right)+\frac{C_{30}+(C_1q_{01}C_{21}/q_{02})}{A_{30}(A_1+\Gamma_1)},$$
$$D_4=\frac{QbC_i(C_1+C_{21})}{q_2q_{02}SA_{30}(A_1+\Gamma_1)},\quad D_5=\frac{C_{30}}{A_{30}}+\frac{C_2+(q_{02}C_{12}/q_{01})}{A_2+\Gamma_2},$$
$$D_6=\frac{b}{A_{30}S}\left(\frac{C_3}{g_3}+\frac{q_{03}}{q_{01}}C_i\right)+\frac{C_{30}[C_2+(q_{02}C_{12}/q_{01})]}{A_{30}(A_2+\Gamma_2)},\quad D_7=\frac{D_1D_4g_1}{g_2},$$
$$C_{13}=C_{23}=C_i,\quad C_1=C_{12}+C_i,\quad C_2=C_{21}+C_i,\quad C_3=(g_1+g_2)C_i,$$
$$q_{0k}=\frac{Q_{0k}}{g_k},\quad b=\exp\left(\frac{\Delta E_{23}}{kT_e}\right),\quad S=2\left(\frac{mkT_e}{2\pi\hbar^2}\right)^{3/2},\quad Q=Q_{01}+Q_{02}+Q_{03}.$$

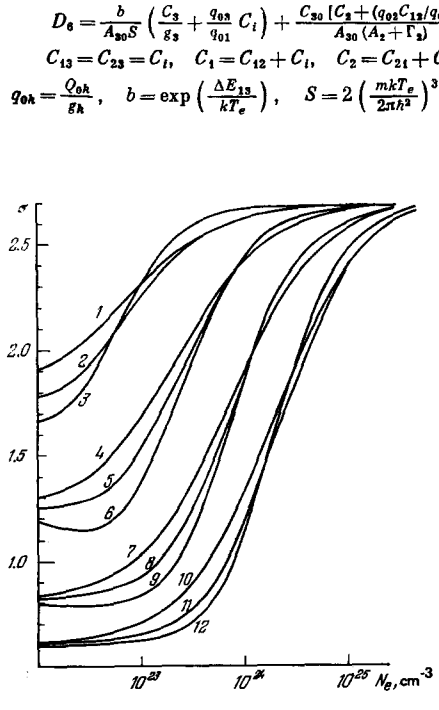

FIG. 24. Plots of $\sigma(N_e)$ for the following ions: OVII (1–3) (kT_e=41, 81, 121 eV), NeIX (4–6) (kT_e=67, 134, 201 eV), MgXI (7–9) (kT_e=100, 200, 300 eV), SiXIII (10–12) (kT_e=140, 280, 420 eV).

Equation (5.2) can be used to determine the intensity ratio for any pair of lines, one of which begins from the triplet and the other from the singlet state. For example, Fig. 24 shows $\sigma=I_T/I_S$ as a function of N_e, calculated from (5.2) for the following ions: OVII, NeIX, MgXI, and SiXIII; I_T is the sum of the intensities of several closely lying triplet lines and I_S is the intensity of the stronger singlet line (in our view, these are the most convenient quantities for experimental determination), namely: $I_S=I(2p^2\ ^1D_2-1s2p\ ^1P_1)$; $I_T=I(2p^2\ ^3P_1-1s2p\ ^3P_0)+\sum_{J=0}^{2}[I(2p^2\ ^3P_J-1s2p\ ^3P_1)+I(2s2p\ ^3P_J-1s2s\ ^3S_1)]+\sum_{J=1}^{2}I(2p^2\ ^3P_J-1s2p\ ^3P_2)$. It is clear from Fig. 24 that the $\sigma(N_e)$ graphs can be used as a basis for density measurements in the range $N_e\sim10^{22}$–10^{25} cm^{-3} in the case of ions with ionization potentials $I_i\sim0.74$–2.4 keV. We note that the drop in the intensity ratio decreases with decreasing charge on the ions. This complicates the diagnostics based on lines of elements lighter than oxygen, i.e., studies of plasmas with still lower temperature (Fig. 24).

6. RANGE OF APPLICATION OF SPECTROSCOPIC METHODS IN PLASMA DIAGNOSTICS

The intensity ratios which we have discussed for a number of spectral lines of multiply-charged ions can be used with suitable ion charges to determine the plasma density in the broad range between $N_e\sim10^{18}$ cm^{-3} and $N_e\sim10^{25}$ cm^{-3} (see Table I). Calculations that have been performed were based on the following three conditions which, in general, may restrict their range of application:

1) the stationary set of equations for the populations is solved

2) the ionization state of the plasma is assumed to correspond to the given temperature and density

3) the plasma is assumed to be optically thin (at any rate, for the particular lines).

Let us consider these conditions in detail.

The time necessary to establish the time-independent ionization state, i.e., the time to establish stationary concentrations of ions in the ground state is usually much longer than the corresponding time for the excited state. At the same time, the plasma may be recombining, overcooling, overheating, or underionized. The degree of deviation from the ionization equilibrium in the case of plasma containing helium-like ions can be determined from the intensities of satellites of the corresponding resonance line.[47] If the departure from the stationary ionization state is considerable, the above computational schemes require slight modification through the inclusion of excitation from inner shells in

TABLE I. Ranges of validity of spectroscopic methods for plasma diagnostics

Method for determining density from intensity ratio	Ion charge	Ionization potential, keV	Diagnostic range, cm^{-3}
Components of resonance doublet of a hydrogen-like ion	11–15	1.96–3.49	10^{20}–10^{22}
Resonance and intercombinational lines of a helium-like ion	9–16	1.47–4.12	10^{19}–10^{23}
Dielectronic satellites of a resonance line of a hydrogen-like ion	9–14	1.47–3.22	10^{20}–10^{23}
	6–12	0.74–2.44	10^{22}–10^{24}
Lines of an oxygen-like ion	12–18	0.73–1.46	10^{18}–10^{20}

the pumping terms for underionized plasma and recombination processes in the case of cooling plasma.

Exact allowance for radiation trapping in the multilevel system is very complicated. This can be done approximately by using the effective radiative decay probabilities introduced by Holstein and Biberman.[112,113] This kind of analysis shows that, in some cases, large optical thickness of the plasma will have no effect on the relative intensity of the spectral lines. For example, large optical thickness in the resonance line of a helium-like ion does not, up to a certain limit, affect the intensity ratio of the resonance and intercombinational lines (see Sec. 4b). In this case, resonance line trapping begins to have an appreciable effect on the intensity only when the effective decay probability of the 2^1P_1 level falls down to a value comparable with the decay probability of the triplet 2^3P_1 level. For ions with $Z \sim 10-20$, this correspond to optical thicknesses $\tau_{opt} \sim 100-10$. In other cases (see Secs. 4a–d and 5), radiation trapping may have an important effect even for $\tau_{opt} \sim 1$ (see, for example, Ref. 114). Reliable diagnostics of nonhomogeneous plasma by the method discussed in Chaps. 4 and 5 is therefore possible only for optically thin plasmas. We note, however, that: (1) in practice, this can be readily achieved by introducing the necessary elements into the composition of the target in the form of small impurities and (2) in the case of dielectronic satellites (Secs. 4c and 5), when the lower level involved in the radiative transition is an excited state, the optical thickness of the plasma in all real experiments is less than unity, and there is no radiation trapping.

In conclusion, we note that the methods for the determination of plasma densities, discussed in Sec. 4, are now quite widely used for dense plasma[23,25,40,42,80-90,95,96,108,115,116] and, as a rule, yield results that are in good agreement with one another and with determinations of the density from the Stark broadening of the lines of hydrogen-like ions (Refs. 40, 42, 88, 90, 95, 96, and 116).

7. EFFECT OF ELECTRIC AND MAGNETIC FIELDS ON THE EMISSION SPECTRA OF MULTIPLY-CHARGED IONS

Strong electric and magnetic fields have an important effect on the nature of the gas-dynamic expansion and compression of inertial plasma.[117,118] This effect has been examined in many theoretical and experimental papers. For example, even the linear theory, as applied to inhomogeneous laser plasmas, predicts a sharp increase in the amplitude of the electric field near the critical point at the laser frequency when the radiation is sharply focused and is polarized in the plane of incidence. An increase in the field amplitude is accompanied by resonance absorption of the laser radiation,[119,120] the presence of which has been confirmed experimentally.[121,122] The characteristic size of inhomogeneities near the critical point is only a few microns,[121] and this is explained by the ponderomotive effects of strong electric fields. Next, the nonlinear theory predicts that electromagnetic oscillations develop at a series of frequencies in the presence of a powerful laser field, which corresponds to parametric instability.[123] Experimental confirmation of such fields would throw considerable light on the nature of electrodynamic processes near the critical point.

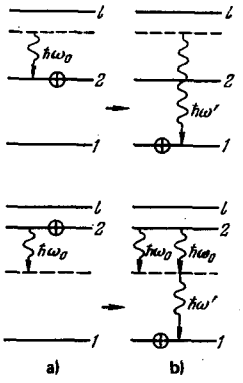

FIG. 25. (a) Raman scattering by excited ions with initial state $B^* + \hbar\omega_0$ and final state $B + \hbar\omega_0'$; (b) stimulated two-photon emission corresponding to initial state $B^* + \hbar\omega_0$ and final state $B + 2\hbar\omega_0 + \hbar\omega_0'$.

We now have the natural question: what conclusions about the presence of electromagnetic fields can be drawn from an analysis of the x-ray line spectrum?

A strong electric field at the laser frequency ω_0 should lead to the appearance of two lines near each parity-forbidden transition ω_{21}[3)] (see Fig. 25). These lines have frequencies $\omega_{21} \pm \omega_0$ and correspond to two-photon processes, namely, anti-Stokes Raman scattering and stimulated two-photon emission. In the absence of random resonances, the line intensities are practically equal and given by

$$I = \frac{(\omega'/\omega_0) N_a \sigma E^2}{8\pi C},$$

where σ is the Raman scattering cross section which, in the approximation of a single virtual state, is given by

$$\sigma = \sigma_T \frac{\omega_0 \omega'^3 (\omega_{12} + \omega_{11}) f_{11} f_{21}}{4 (\omega_{12} - \omega_0)^2 (\omega_{11} + \omega_0)^2 \omega_{11} \omega_{12}},$$

$$\sigma_T = \frac{8\pi}{3} \left(\frac{e^2}{mc^2} \right)^2,$$

where $\omega' = \omega_{21} \pm \omega_0$, σ_T is the Thomson cross section, and f_{ij} is the $i \to j$ oscillator strength. It has been shown[124] that the intensity of these laser satellites begins to be comparable with the intensities of allowed lines due to helium-like and lithium-like ions for $cE^2/8\pi \approx 10^{15}$ W/cm^2. The satellite splitting $2\omega_0$ amounts to about 2 eV in the case of the neodymium laser, which is in agreement with the experimental spectral resolution in the region above a few angstroms. For the CO_2 laser, the splitting $2\omega_0$ is already less than the spectral resolution. Laser satellites should then be observed simply as lines with the forbidden transition frequency. Ion-ion collisions in very dense plasmas should lead to an analogous effect.[125] Lines corresponding to forbidden transitions have been reported for laser plasmas.[126]

Spontaneous magnetic fields have been detected during

[3)] This effect was considered by Baranger and Moser.[138]

the focusing of laser radiation both on the surfaces of solids and in gases.[127-129] Faraday rotation has been used[129] to record fields of the order of a few megagauss. However, attempts to observe the Zeeman splitting of spectral lines in laser plasmas have so far been unsuccessful. This problem remains the testing ground for spectroscopic diagnostics.[130,131]

The size of the Zeeman splitting for fields of the order of 10^6 G (this corresponds to contemporary theoretical ideas[130,132,133]) is[134] $\Delta\omega_H = eH/2mc^2$ eV. The Doppler width of spectral lines depends on the flux and conditions of focusing, and lies in the range $\Delta\omega_D/\omega \sim 10^{-3}-10^{-4}$. We shall take $\Delta\omega_D/\omega = 5\times 10^{-4}$ as a typical value. Reliable observation of the splitting is possible for $\Delta\omega_H > \Delta\omega_D$, i.e., for $\hbar\omega < 60$ eV. Transitions of the form $2^3P - 2^3S$ in helium-like ions are very convenient for this purpose. These lines can readily be identified and, moreover, when $N_e \sim 10^{20}-10^{21}$ cm^{-3}, their intensity is much higher than, for example, the intensity of the $2^1P - 2^1F$ line because the 2^3P state is metastable (see Sec. 4b). In the case of MgXI and SiXIII, the corresponding wavelengths are 950.6 and 763.36 Å, respectively. Systematic spectral studies of hot laser plasmas in this range have not so far been carried out.

8. CONCLUSIONS

Studies of x-ray line spectra emitted by inertially confined systems are thus capable of yielding extensive information on the fundamental properties of multiply-charged ions of elements introduced into the targets, and on the physical conditions obtaining in plasmas. Successful development of techniques for producing spectra with the necessary time and spatial resolution will make x-ray spectroscopy one of the most effective methods of plasma diagnostics. The development of such methods for the investigation of inertially confined plasmas has assumed an importance on a par with that of the development of x-ray microscopy and neutron diagnostics.[135,136]

The authors are indebted to N. G. Basov and I. I. Sobel'man, who read the manuscript and made a number of valuable suggestions, and to S. A. Pikus, E. N. Ragozin, and A. Ya. Faenov for providing experimental data.

[1]N. G. Basov and O. N. Krokhin, Zh. Eksp. Teor. Fiz. **46**, 171 (1964) [Sov. Phys. JETP **19**, 123 (1964)].
[2]N. G. Basov, S. D. Zakharov, P. G. Kryukov, Yu. V. Senatskiĭ, and S. V. Chekalin, Pis'ma Zh. Eksp. Teor. Fiz. **8**, 26 (1968) [JETP Lett. **8**, 14 (1968)].
[3]K. A. Brueckner and S. Jorna, Rev. Mod. Phys. **46**, 325 (1974).
[4]N. G. Basov, V. B. Rozanov, and N. M. Sobolevskii, Izv. Akad. Nauk SSSR Ser. Energ. Transp. No. 6, 3 (1975).
[5]A. A. Filyukov (ed.), Problemy lazernogo tamoyadernogo sinteza (Problems in Laser Thermonuclear Fusion), Collection of Papers, Atomizdat, Moscow (1976).
[6]A. M. Prokhorov, S. I. Anisimov, and P. P. Pashinin, Usp. Fiz. Nauk **119**, 401 (1976) [Sov. Phys. Usp. **19**, 547 (1976)].
[7]Yu. V. Afanas'ev, N. G. Basov, E. G. Gamaliĭ, O. N. Krokhin, and V. B. Rozanov, Priroda No. 10, 5 (1976).
[8]F. Winterberg, Phys. Rev. **174**, 212 (1968).
[9]M. J. Clauser, Phys. Rev. Lett. **34**, 570 (1975).
[10]S. L. Bogolyubskiĭ, B. P. Gerasimov, V. I. Liksonov, A. M. Mikhaĭlov, Yu. P. Popov, L. I. Rudakov, A. A. Samarskiĭ, and V. P. Smirnov, Pis'ma Zh. Eksp. Teor. Fiz. **24**, 206 (1976) [JETP Lett. **24**, 182 (1976)].
[11]Proc. Sixth Conf. on Plasma Physics and Controlled Nuclear Fusion Research, Berchtesgarten, October 6–13, 1976, Nucl. Fus. Suppl. **1**, 167 (1977).
[12]O. A. Gusev, I. M. Roĭfe, and V. I. Engel'ko NIIEA, No. OE-18, L., 1977.
[13]P. A. Miller, R. J. Butler, M. Cowan, J. R. Fruman, J. W. Ponkey, T. P. Wright, and G. Yonas, Phys. Rev. Lett. **39**, 92 (1977).
[14]F. Winterberg, Plasma Phys. **17**, 69 (1975).
[15]M. J. Clauser, Phys. Rev. Lett. **35**, 848 (1975).
[16]M. Grunspan, S. Humprils, J. Maehchem, and R. N. Sudan, *ibid.* **39**, 24 (1977).
[17]L. A. Dushin (Ed.), Zondirovanie neodnorodnoĭ plazmy ėlektromagnitnymi volnami (Probing of Inhomogeneous Plasmas with Electromagnetic Waves), Collection of Papers, Nauka, M., 1973.
[18]E. I. Kuznetsov and D. A. Shcheglov, Metody diagnostiki vysokotemperaturnoĭ plasmy (Diagnostic Methods for High-Temperature Plasmas), Atomizdat, M., 1974.
[19]L. I. Pyatnitskiĭ, Lazernaya diagnostika plazmy (Laser Plasma Diagnostics), Atomizdat, M., 1976.
[20]A. G. Molchanov, Usp. Fiz. Nauk **106**, 165 (1972) [Sov. Phys. Usp. **15**, 124 (1972)].
[21]R. W. Waynant and R. C. Elton, Proc. IEEE **64**, 1059 (1976).
[22]A. V. Vinogradov, I. I. Sobelman, and E. A. Yukov, Invited Paper presented to V VUV Radiation Physics Conf., Montpellier, September 1977.
[23]A. Zigler, H. Zmora, and Y. Komet, Phys. Lett. A **60**, 319 (1977).
[24]J. C. Contourand and C. Faure, Opt. Commun. **17**, 103 (1976).
[25]Yu. A. Kas'yanov, M. A. Mazing, V. V. Chevokin, and A. P. Shchevel'ko, Pis'ma Zh. Eksp. Teor. Fiz. **25**, 373 (1977) [JETP Lett. **25**, 348 (1977)].
[26]A. H. Gabriel and C. Jordan, in: Case Studies in Atomic Collision Physics, Vol. 2, 1972, p. 209.
[27]L. Cohen, U. Feldman, M. Swartz, and J. H. Underwood, J. Opt. Soc. Am. **58**, 843 (1968).
[28]T. N. Lie and R. C. Elton, Phys. Rev. A **3**, 865 (1971).
[29]E. Ya. Gol'ts, I. A. Zhitnik, E. Ya. Kononov, L. S. Mandel'shtam, and Yu. V. Sidel'nikov, Dokl. Akad. Nauk **220**, 560 (1975) [Sov. Phys. Dokl. **20**, 49 (1975)].
[30]W. A. Cilliers, R. U. Datla, and H. R. Griem, Phys. Rev. A **12**, 1408 (1975).
[31]T. N. Lie and R. C. Elton, Bull. Am. Phys. Soc. **21**, 1040 (1976).
[32]N. J. Peacock, R. J. Spear, and M. G. Hobby, J. Phys. B **2**, 798 (1969).
[33]A. H. Gabriel and T. M. Paget, *ibid.* **5**, 673 (1972).
[34]P. G. Burkhalter, C. M. Dozier, and D. J. Nagel, Naval Research Lab. Preprint No. 101, Washington, 1976.
[35]C. M. Dozier, P. G. Burkhalter, D. J. Nagel, S. J. Stephankis, and D. Mosher, J. Phys. B **10**, L73 (1977).
[36]E. V. Aglitskiĭ, V. A. Boĭko, S. M. Zakharov, S. A. Pikuz, and A. Ya. Faenov, Kvantovaya Elektron. (Moscow) **1**, 908 (1974) [Sov. J. Quantum Electron. **4**, 500 (1974)].
[37]D. J. Nagel, P. G. Burkhalter, C. M. Dozier, J. F. Holzrichter, R. M. Klein, J. M. McMahon, J. A. Stamper, and R. R. Whitlock, Phys. Rev. Lett. **33**, 743 (1974).
[38]U. Feldman, G. A. Doshek, D. J. Nagel, R. D. Cowan, and R. R. Whitlock, Appl. Phys. **192**, 213 (1974).
[39]R. G. Burkhalter, D. J. Nagel, and R. D. Cowan, Phys. Rev. A **11**, 782 (1975).

[40]V. A. Boĭko, S. A. Pikuz, and A. Ya. Faenov, Preprints Nos. 17, 19, 20, P. N. Lebedev Physics Institute, Moscow, 1976.
[41]W. E. Behring, L. Cohen, G. A. Doshek, and U. Feldman, J. Opt. Soc. Am. **66**, 376 (1976).
[42]V. A. Boiko, S. A. Pikuz, and A. Ya. Faenov, J. Quant. Spectrosc. Radiat. Transfer **19**, 11 (1978).
[43]U. I. Safronova, *ibid.* **14**, 254 (1974).
[44]A. M. Ermolaev and M. Jones, J. Phys. B **7**, 199 (1974).
[45]E. N. Ivanova and U. I. Safronova, *ibid.* **8**, 1591 (1975).
[46]C. R. Bhalla, A. H. Gabriel, and L. P. Presnyakov, Mon. Not. R. Aston. Soc. **172**, 359 (1975).
[47]L. P. Presnyakov, Usp. Fiz. Nauk **119**, 49 (1976) [Sov. Phys. Usp. **19**, 387 (1976)].
[48]R. Marrus and R. W. Schmieder, Phys. Rev. A **5**, 1160 (1972).
[49]H. Gould, R. Marrus, and P. Mohr, Phys. Rev. Lett. **33**, 676 (1974).
[50]H. Gould, R. Marrus, and R. W. Schmieder, *ibid.* **31**, 504 (1973).
[51]J. R. Mowat, P. M. Griffin, H. H. Haselton, R. Laubert, D. J. Pegg, R. S. Peterson, I. A. Selin, and R. S. Thoe, Phys. Rev. A **11**, 2198 (1975).
[52]P. H. Heckmann, E. Träbert, H. Winter, F. Hannebauer, H. H. Bukow, and H. V. Buttlar, *ibid.* **12**, 126 (1976).
[53]D. J. Pegg, S. B. Elston, P. M. Griffin, H. C. Haydden, J. P. Forester, P. S. Thoe, R. S. Peterson, and I. A. Selin, *ibid.* **14**, 1036 (1976).
[54]R. U. Datla, M. Blaha, and H. J. Kunze, *ibid.* **12**, 1076 (1975).
[55]R. U. Datla, L. J. Nugent, and H. R. Griem, *ibid.* **14**, 976 (1976).
[56]G. W. F. Drake and A. Dalgarno, Astrophys. J. **157**, 459 (1969).
[57]L. A. Vaĭnshteĭn and U. I. Safronova, Preprint No. 6, P. N. Lebedev Physics Institute, Moscow, 1975.
[58]L. A. Vaĭnshteĭn, I. I. Sobel'man, and E. A. Yukov, Sechenіya vozbuzhdeniya atomov i ionov élektronami (Cross Sections for the Excitation of Atoms and Ions by Electron Impact), Nauka, M., 1973.
[59]W. R. Johnson, D. C. Lin, and A. Dalgarno, J. Phys. B **2**, L301 (1976).
[60]E. J. Kelsey, Ann. Phys. **98**, 462 (1976).
[61]L. A. Vaĭnshteĭn and V. P. Shevel'ko, Preprint No. 87, P. N. Lebedev Institute of Physics, Moscow, 1970; No. 26, 1974.
[62]W. Eissner and M. J. Seaton, J. Phys. B **5**, 2187 (1972).
[63]M. J. Seaton, *ibid.* **7**, 1817 (1974).
[64]M. J. Seaton, in: Atomic and Molecular Processes, ed. by D. R. Bates, Academic Press, N. Y., 1962; Proc. Phys. Soc. London **79**, 1105 (1962).
[65]H. Van Regemorter, Astrophys. J. **136**, 906 (1962).
[66]W. L. Wiese and A. W. Weise, An Assessment of the Effective Gaunt Factor Approximation, NBS, Preprint, 1977.
[67]K. Alder, A. Bohr, T. Huus, B. Mottelson, and A. Wonter, Rev. Mod. Phys. **28**, 432 (1956).
[68]L. Spitzer, Phys. Rev. **58**, 348 (1940).
[69]M. J. Seaton, Proc. Phys. Soc. London **77**, 174 (1961).
[70]M. I. Chibisov, Opt. Spektrosk. **27**, 9 (1969) [Opt. Spectrosc. (USSR) **27**, 4 (1969)].
[71]V. S. Lisitsa and G. V. Sholin, Zh. Eksp. Teor. Fiz. **61**, 912 (1971) [Sov. Phys. JETP **34**, 484 (1972)].
[72]V. S. Lisitsa, Usp. Fiz. Nauk **122**, 449 (1977) [Sov. Phys. Usp. **120**, 603 (1977)].
[73]L. A. Vaĭnshteĭn and A. V. Vinogradov, J. Phys. B **3**, 1090 (1970).
[74]V. P. Shevelko, A. M. Urnov, and A. V. Vinogradov, *ibid.* **9**, 2859 (1976).
[75]V. P. Shevelko, I. Yu. Skobelev, and A. V. Vinogradov, Phys. Scripta **16**, 123 (1977).
[76]I. Yu. Skobelev and A. V. Vinogradov, J. Phys. B **11**, 2899 (1978).
[77]A. V. Vinogradov, I. Yu. Skobelev, and E. A. Yukov, Fiz. Plazmy **3**, 686 (1977) [Sov. J. Plasma Phys. **3**, 389 (1977)].
[78]I. I. Sobel'man and E. L. Feĭnberg, Zh. Eksp. Teor. Fiz. **34**, 494 (1958) [Sov. Phys. JETP **7**, 339 (1958)].
[79]A. V. Vinogradov, I. I. Sobel'men, and E. A. Yukov, Kvantovaya Elektron. (Moscow) **1**, 268 (1974) [Sov. J. Quantum Electron. **4**, 149 (1974)].
[80]E. A. Asmaryan and Yu. L. Klimontovich, Vestn. Mosk. Univ. Fiz. **3**, 273 (1974).
[81]J. C. Weisheit and B. W. Shore, Astrophys. J. **194**, 519 (1974).
[82]J. C. Weisheit, J. Phys. B **8**, 2556 (1975).
[83]J. C. Weisheit and B. F. Rozsnyai, *ibid.* **9**, L63 (1976).
[84]A. V. Vinogradov and V. P. Shevel'ko in: Abstracts of Papers of 12th ICPIG, Part 1, Eindhoven, Holland, 1975, p. 261.
[85]A. V. Vinogradov and V. N. Shevel'ko Zh. Eksp. Teor. Fiz. **71**, 1037 (1976) [Sov. Phys. JETP **44**, 542 (1976)].
[86]A. I. Akhiezer (ed.), Elektrodinamika Plazmy (Electrodynamics of Plasmas), Nauka, M., 1974.
[87]G. W. F. Drake, G. A. Victor, and A. Dalgarno, Phys. Rev. **180**, 25 (1969).
[88]V. A. Boĭko, A. V. Vinogradov, S. A. Pikuz, I. Yu. Skobelev, A. Ya. Faenov, and E. A. Yukov, Fiz. Plazmy **4**, 97 (1978) [Sov. J. Plasma Phys. **4**, 54 (1978)].
[89]H. J. Kunze, A. H. Gabriel, and H. R. Griem, Phys. Rev. **165**, 267 (1968).
[90]E. V. Aglitskiĭ, V. A. Boĭko, A. V. Vinogradov, and E. A. Yukov, Kvantovaya Elektron. (Moscow) **1**, 579 (1974) [Sov. J. Quantum Electron. **4**, 322 (1974)].
[91]A. V. Vinogradov, I. Yu. Skobelev, and E. A. Yukov, Kvantovaya Elektron. (Moscow) **2**, 1165 (1975) [Sov. J. Quantum Electron. **5**, 630 (1975)].
[92]L. A. Vaĭnshteĭn, Zh. Eksp. Teor. Fiz. **67**, 63 (1974) [Sov. Phys. JETP **40**, 32 (1975)].
[93]A. V. Vinogradov, I. Yu. Akobelev, I. I. Sobel'man, and E. A. Yukov, Kvantovaya Elektron. (Moscow) **2**, 2189 (1975) [Sov. J. Quantum Electron. **5**, 1192 (1975)].
[94]A. V. Vinogradov, I. Yu. Akobelev, and E. A. Yukov, Kvantovaya Elektron (Moscow) **3**, 981 (1976) [Sov. J. Quantum Electron. **6**, 525 (1976)].
[95]V. A. Boĭko, A. V. Vinogradov, S. A. Pikuz, I. Yu. Skobelev, A. Ya. Faenov, and E. A. Yukov, J. Phys. B **10**, 3387 (1977).
[96]V. I. Bayanov, V. A. Boĭko, A. V. Vinogradov, S. S. Gulidov, A. A. Ilyukhin, V. A. Katulin, A. A. Mak, V. Yu. Nosach, A. L. Petrov, G. V. Peregudov, S. A. Pikuz, I. Yu. Skobelev, A. D. Strikov, A. Ya. Faenov, V. A. Chirkov, and E. A. Yukov, Pis'ma Zh. Eksp. Teor. Fiz. **24**, 352 (1976) [JETP Lett. **24**, 319 (1976)].
[97]A. V. Vinogradov, I. Yu. Skobelev, and E. A. Yukov, Zh. Eksp. Teor. Fiz. **72**, 1762 (1977) [Sov. Phys. JETP **45**, 925 (1977)].
[98]B. C. Fawcett, Atom. Data and Nucl. Data Tables **16**, 135 (1975).
[99]E. Ya. Kononov, V. I. Kovalev, A. N. Ryabtsev, and S. S. Churilov, Kvantovaya Elektron. (Moscow) **4**, 190 (1977) [Sov. J. Quantum Electron. **7**, 111 (1977)].
[100]G. A. Doshek, U. Feldman, J. Davis, and R. D. Cowan, Phys. Rev. A **12**, 980 (1975).
[101]R. C. Elton, Appl. Opt. **14**, 97 (1975).
[102]A. N. Zherikhin, K. N. Koshelev, and C. S. Letokhov, Kvantovaya Elektron. (Moscow) **3**, 152 (1976) [Sov. J. Quantum Electron. **6**, 82 (1976)].
[103]J. Davis and K. G. Whitney, Appl. Phys. Lett. **29**, 419 (1976).
[104]A. V. Vinogradov, I. I. Sobel'man, and E. A. Yukov, Kvantovaya Elektron. (Moscow) **4**, 63 (1977) [Sov. J. Quantum Electron **7**, 32 (1977)].
[105]L. A. Vaĭnshteĭn, A. V. Vinogradov, U. I. Safronova, and I. Yu. Skobelev, Kvantovaya Elektron. (Moscow) **5**, 417 (1978) [Sov. J. Quantum Electron. **8**, 239 (1978)].
[106]L. J. Palumbo and R. C. Elton, J. Opt. Soc. Am. **67**, 480

(1977).
[107]A. A. Ilyukhin, G. V. Peregudov, E. N. Ragozin, I. I. Sobel'man, and V. A. Chirkov, Pis'ma Zh. Eksp. Teor. Fiz. **25**, 586 (1977) [JETP Lett. **25**, 550 (1977)].
[108]A. V. Vinogradov, G. V. Peregudov, E. N. Ragozin, I. Yu. Skobelev, and E. A. Yukov, Kvantovaya Elektron. (Moscow) **5**, 1077 (1978) [Sov. J. Quantum Electron. **8**, 615 (1978)].
[109]I. L. Beĭgman, L. A. Vaĭnshteĭn, and A. V. Vinogradov, Preprint No. 5, P. N. Lebedev Institute of Physics, Moscow, 1967.
[110]I. Yu. Skobelev, A. V. Vinogradov, and E. A. Yukov, Phys. Scripta **18**, 78 (1978).
[111]A. V. Vinogradov, and I. Yu. Skobelev, Pis'ma Zh. Eksp. Teor. Fiz. **27**, 97 (1978) [JETP Lett. **27**, 88 (1978)].
[112]L. M. Biberman, Zh. Eksp. Teor. Fiz. **17**, 419 (1947).
[113]V. V. Ivanov, Perenos izlucheniya i spektry nebesnykh tel (Radiative Transport and the Spectra of Celestial Bodies), Nauka, M., 1966.
[114]I. L. Beĭgman, V. A. Boĭko, S. A. Pikuz, and A. Ya. Faenov, Zh. Eksp. Teor. Fiz. **71**, 975 (1976) [Sov. Phys. JETP **44**, 511 (1976)].
[115]B. Yaakobi and A. Nee, Phys. Rev. Lett. **36**, 1077 (1976).
[116]V. A. Boĭko, S. A. Pikuz, and A. Ya. Faenov, Preprint No. 26, P. N. Lebedev Physics Institute, Moscow, 1977.
[117]K. A. Brueckner and R. S. Janda, Nucl. Fusion **17**, 451 (1977); P. Mulser and C. Van Kessel, Phys. Rev. Lett. **38**, 902 (1977).
[118]D. G. Colombant, K. G. Whitney, D. A. Tidman, N. K. Winzer, and J. Davis Phys. Fluids **18**, 1687 (1975).
[119]A. V. Vinogradov and V. V. Pustovalov, Pis'ma Zh. Eksp. Teor. Fiz. **13**, 317 (1971) [JETP Lett. **13**, 226 (1971)].
[120]J. P. Freidgerb, R. W. Mitchell, R. L. Morse, and L. J. Rudzinski, Phys. Rev. Lett. **28**, 795 (1972).
[121]J. S. Pearlmann, J. J. Tomson, and C. E. Max, *ibid.* **38**, 1397 (1977).
[122]J. S. Pearlmann and M. Keith Matzen, *ibid.* **39**, 140 (1977).
[123]V. P. Silin, Parametricheskoe vozdeĭstvie izlucheniya bol'shoi moshchnosti na plazmu (Parametric Effect of High Power Radiation on Plasmas), Nauka, M., 1973.
[124]A. V. Vinogradov and E. A. Yukov, Kvantovaya Elektron. (Moscow) **2(14)**, 105 (1973) [Sov. J. Quantum Electron. **5**, 59 (1973)].
[125]A. V. Vinogradov and E. A. Yukov, Fiz. Plazmy **1**, 860 (1975) [Sov. J. Plasma Phys. **1**, 472 (1975)].
[126]R. J. Dewhurst, Opt. Commun. **12**, 60 (1974).
[127]V. V. Korobkin and R. V. Serov, Pis'ma Zh. Eksp. Teor. Fiz. **4**, 103 (1966) [JETP Lett. **4**, 70 (1966)].
[128]G. A. Askar'yan, M. S. Rabinovich, A. D. Smirnov, and V. B. Studenov, Pis'ma Zh. Eksp. Teor. Fiz. **5**, 116 (1967) [JETP Lett. **5**, 93 (1967)].
[129]J. A. Stamper and B. H. Rippin, Phys. Rev. Lett. **34**, 138 (1975).
[130]J. A. Stamper and B. H. Rippin, in: NRL Memorandum Report 3315, August 1976, p. 92.
[131]P. Jaegle, Invited Paper presented to Fifth VUV Radiation Physics Conf., Montpellier, September 1977.
[132]L. A. Bol'shov, Yu. A. Dreĭzen, and A. M. Dykhne, Pis'ma Zh. Eksp. Teor. Fiz. **19**, 288 (1974) [JETP Lett. **19**, 168 (1974)].
[133]B. A. Al'terkop, E. V. Mishin, and A. A. Rukhadze, Pis'ma Zh. Eksp. Teor. Fiz. **19**, 291 (1974) [JETP Lett. **19**, 170 (1974)].
[134]I. I. Sobel'man, Vvedenie v teoriyu atomnykh spektrov (Introduction to the Theory of Atomic Spectra) Fizmatgiz., M., (1963); Pergamon Press, Oxford, 1972.
[135]E. G. Gamaliĭ, S. Yu. Gus'kov, and N. M. Sobolevskiĭ, Tr. Fiz. Inst. Akad. Nauk SSSR **97**, 10 (1977).
[136]O. N. Krokhin, F. A. Nikolaev, and G. V. Sklizkov, Pis'ma Zh. Eksp. Teor. Fiz. **19**, 389 (1974) [JETP Lett. **19**, 214 (1974)].
[137]V. A. Boiko, A. Yu. Chugunov, A. Ya. Faenov, S. A. Pikuz, I. Yu. Skobelev, A. V. Vinogradov, and E. A. Yukov, J. Phys. B **12**, 213 (1979).
[138]M. Baranger and B. Moser, Phys. Rev. **123**, 25 (1961).

Translated by S. Chomet